Human Molecular Genetics, 2019, Vol. 28, No. 15 2531–2548

doi: 10.1093/hmg/ddz075
Advance Access Publication Date: 15 April 2019
General Article

GENERAL ARTICLE

The protective variant rs7173049 at *LOXL1* locus impacts on retinoic acid signaling pathway in pseudoexfoliation syndrome

Daniel Berner[1], Ursula Hoja[1], Matthias Zenkel[1], James Julian Ross[1], Steffen Uebe[2], Daniela Paoli[3], Paolo Frezzotti[4], Robyn M. Rautenbach[5], Ari Ziskind[5], Susan E. Williams[6], Trevor R. Carmichael[6], Michele Ramsay[7], Fotis Topouzis[8], Anthi Chatzikyriakidou[9], Alexandros Lambropoulos[9], Periasamy Sundaresan[10], Humaira Ayub[11], Farah Akhtar[12], Raheel Qamar[13], Juan C. Zenteno[14,15], Marisa Cruz-Aguilar[14], Yury S. Astakhov[16], Michael Dubina[16,17], Janey Wiggs[18], Mineo Ozaki[19,20], Friedrich E. Kruse[1], Tin Aung[21,22,23], André Reis[2], Chiea Chuen Khor[21,24,25,†], Francesca Pasutto[2,†] and Ursula Schlötzer-Schrehardt[1,†,*]

[1]Department of Ophthalmology, Universitätsklinikum Erlangen, Friedrich-Alexander-Universität Erlangen-Nürnberg, Erlangen 91054, Germany, [2]Institute of Human Genetics, Universitätsklinikum Erlangen, Friedrich-Alexander-Universität Erlangen-Nürnberg, Erlangen 91054, Germany, [3]Department of Ophthalmology, Monfalcone Hospital, Gorizia, 34074, Italy, [4]Ophthalmology Unit, Department of Medicine, Surgery and Neuroscience, University of Siena, Siena, 53100, Italy, [5]Division of Ophthalmology, Stellenbosch University and Tygerberg Hospital, Cape Town 7505, South Africa, [6]Division of Ophthalmology, University of the Witwatersrand, Johannesburg 2193, South Africa, [7]Sydney Brenner Institute for Molecular Bioscience, Faculty of Health Sciences, University of the Witwatersrand, Johannesburg 2193, South Africa, [8]Department of Ophthalmology, School of Medicine, Aristotle University of Thessaloniki, 54636, Thessaloniki, Greece, [9]Department of Biology and Genetics, School of Medicine, Aristotle University of Thessaloniki, Thessaloniki, 54124, Greece, [10]Dr. G.Venkataswamy Eye Research Institute, Aravind Medical Research Foundation, Aravind Eye Hospital, Madurai, 625020, India, [11]Department of Environmental Sciences, COMSATS Institute of Information Technology, Abbottabad, 22010, Pakistan, [12]Pakistan Institute of Ophthalmology, Al-Shifa Trust Eye Hospital, Rawalpindi, 46000, Pakistan, [13]Department of Biosciences, COMSATS Institute of Information Technology, Islamabad, 45550, Pakistan, [14]Genetics Department, Institute of Ophthalmology 'Conde de Valenciana', Mexico City, 06726, Mexico,

[†]These authors contributed equally to this work.
Received: December 13, 2018. **Revised:** March 29, 2019. **Accepted:** April 1, 2019

[15]Biochemistry Department, Faculty of Medicine, National Autonomous University of Mexico, Mexico City, 04510, Mexico, [16]Department of Ophthalmology, Pavlov First Saint Petersburg State Medical University, St Petersburg 197022, Russia, [17]St Petersburg Academic University, St Petersburg 194021, Russia, [18]Department of Ophthalmology, Harvard Medical School, Massachusetts Eye and Ear Infirmary, 02114 Boston, Massachusetts, USA, [19]Ozaki Eye Hospital, Hyuga, Miyazaki, 882-0056, Japan, [20]Department of Ophthalmology, Faculty of Medicine, University of Miyazaki, Miyazaki, 889-1692, Japan, [21]Singapore Eye Research Institute, 168751 Singapore, [22]Singapore National Eye Center, 168751 Singapore, [23]Department of Ophthalmology, Yong Loo Lin School of Medicine, National University of Singapore, 119228 Singapore, [24]Genome Institute of Singapore, 138672 Singapore, and [25]Department of Biochemistry, Yong Loo Lin School of Medicine, National University of Singapore, 117596 Singapore

*To whom correspondence should be addressed at: Department of Ophthalmology, University of Erlangen-Nürnberg Schwabachanlage 6, Erlangen 91054, Germany. Tel: +49 91318534433; Fax: +49 91318534631; Email: Ursula.schloetzer-schrehardt@uk-erlangen.de

Abstract

LOXL1 (lysyl oxidase-like 1) has been identified as the major effect locus in pseudoexfoliation (PEX) syndrome, a fibrotic disorder of the extracellular matrix and frequent cause of chronic open-angle glaucoma. However, all known PEX-associated common variants show allele effect reversal in populations of different ancestry, casting doubt on their biological significance. Based on extensive *LOXL1* deep sequencing, we report here the identification of a common non-coding sequence variant, rs7173049A>G, located downstream of *LOXL1*, consistently associated with a decrease in PEX risk (odds ratio, OR = 0.63; $P = 6.33 \times 10^{-31}$) in nine different ethnic populations. We provide experimental evidence for a functional enhancer-like regulatory activity of the genomic region surrounding rs7173049 influencing expression levels of *ISLR2* (immunoglobulin superfamily containing leucine-rich repeat protein 2) and *STRA6* [stimulated by retinoic acid (RA) receptor 6], apparently mediated by allele-specific binding of the transcription factor thyroid hormone receptor beta. We further show that the protective rs7173049-G allele correlates with increased tissue expression levels of *ISLR2* and *STRA6* and that both genes are significantly downregulated in tissues of PEX patients together with other key components of the STRA6 receptor-driven RA signaling pathway. siRNA-mediated downregulation of RA signaling induces upregulation of *LOXL1* and PEX-associated matrix genes in PEX-relevant cell types. These data indicate that dysregulation of STRA6 and impaired retinoid metabolism are involved in the pathophysiology of PEX syndrome and that the variant rs7173049-G, which represents the first common variant at the broad *LOXL1* locus without allele effect reversal, mediates a protective effect through upregulation of STRA6 in ocular tissues.

Introduction

Pseudoexfoliation (PEX) syndrome is a common, late-onset systemic disorder of the extracellular matrix affecting virtually all populations worldwide with prevalence rates varying from 5 to 30% of persons over 60 years of age (1). It is characterized by the excessive production of an abnormal, highly cross-linked, fibrillar material that progressively accumulates throughout the anterior eye segment and various organ systems (2,3). These abnormal matrix deposits may obstruct the aqueous humor outflow pathways and lead to chronic intraocular pressure elevation and subsequent glaucomatous optic nerve damage in about 30% of patients (4). Overall, PEX syndrome is considered to be the most common identifiable cause of glaucoma worldwide accounting for 25% up to 70% of open-angle glaucoma in some countries (5). Owing to the systemic nature of the underlying matrix process, PEX syndrome has also been associated with cardiovascular disease, aortic aneurysms and a spectrum of connective tissue diseases such as pelvic organ prolapse and inguinal hernias (6–9). The prevalence of PEX syndrome and its associated ocular and systemic complications markedly increase with age, constituting a growing medical burden (1).

The etiology of PEX syndrome is incompletely understood, but a multifactorial complex model combining polygenic inheritance with environmental factors, such as geographic latitude and UV exposure, has been suggested (10,11). *LOXL1 (lysyl oxidase-like 1)*, coding for a cross-linking matrix enzyme, was the first major susceptibility gene identified for PEX syndrome/glaucoma through a genome-wide association study (GWAS) in a relatively small sample size of 75 PEX cases only (12). Two common non-synonymous coding variants in exon 1, p.R141L (rs1048661G>T) and p.G153D (rs3825942G>A), and one intronic variant (rs2165241T>C) were found to confer a 20-fold increased risk for disease. This exceptionally strong association has been irrefutably replicated in multiple populations worldwide (13,14), but involved consistent allele effect reversal between Caucasians and other ethnic groups (10). Further search at the *LOXL1* locus led to the identification of additional PEX-associated variants in the promoter and intron 1 of *LOXL1*, which were shown to regulate expression levels of both *LOXL1* and *LOXL1-AS1* (*LOXL1, antisense RNA 1*), a long non-coding RNA (15–17). However, all hitherto identified, coding and regulatory PEX-associated variants in *LOXL1* are flipped between populations of different ancestry, casting doubt on their causative roles in disease pathogenesis and prompting further search for additional genetic variants.

A large-scale GWAS performed by a worldwide consortium on 13 838 cases and 110 275 controls not only identified six novel PEX-associated loci (*CACNA1A, POMP, TMEM136, AGPAT1, RBMS3 and SEMA6A*) with modest effect sizes only (odds ratio,

OR = 1.14–1.17) but also confirmed an overwhelming association of *LOXL1* (OR = 9.87; $P = 2.13 \times 10^{-217}$) (18). Deep resequencing of the *LOXL1* locus, conducted in 5566 cases and 6279 controls, not only reconfirmed allele reversal at rs3825942 and rs1048661 but also confirmed the lack of any single unflipped common variant in the intragenic region of *LOXL1* that was consistently associated with PEX across populations and that surpassed genome-wide significance levels (18). The rare protective *LOXL1* p.Y407F variant identified in this effort was only found in Japanese and, due to its rarity, only explained a small fraction of the association at rs3825942.

According to current knowledge, *LOXL1* not only exerts the strongest genetic effect among all known susceptibility genes for PEX syndrome/glaucoma but also appears to have a key role in disease pathogenesis (19,20). *LOXL1* encodes lysyl oxidase homolog 1, a member of the lysyl oxidase family of monoamine oxidases that catalyze the generation of lysine-derived covalent cross-links in extracellular matrix molecules such as collagen and elastin (ELN) (21). Dysregulated expression of LOXL1 in tissues of PEX patients has been suggested to contribute to cross-linking of ELN and fibrillin in the formation of fibrillar PEX aggregates on the one hand. On the other hand, it has also been shown to be causatively involved in elastotic-degenerative connective tissue alterations predisposing to glaucoma and systemic complications (22). However, a substantial gap remains between the strength of association, the genome-wide significant allele effect reversal and our understanding of how associated variants contribute to disease.

Therefore, the aim of this study was to refine the genetic landscape at *LOXL1* locus by extending the genetic analysis to intergenic regions flanking *LOXL1*, in order to potentially identify unflipped causal risk variants with functional effects on gene regulation. We detected a single common non-coding sequence variant, rs7173049A>G, downstream of *LOXL1*, with the minor allele G being consistently enriched in controls across all populations studied, translating to a potentially significant protective, biological effect. Functional assays provided evidence for a regulatory activity of the genomic region surrounding rs7173049, influencing expression levels of two genes in *cis*, *STRA6* [stimulated by retinoic acid (RA) receptor 6] and *ISLR2* (immunoglobulin superfamily containing leucine-rich repeat protein 2). Using electrophoretic mobility shift and supershift assays guided by *in silico* predictions of putative transcription factor binding motifs, we further showed specific binding of transcription factor THRβ (thyroid hormone receptor beta) to DNA sequences containing the protective rs7173049-G allele. The presence of the G allele was also found to correlate with increased tissue expression levels of *STRA6* and *ISLR2*, which both were significantly downregulated in ocular tissues of PEX patients together with other key components of the STRA6 receptor-driven RA signaling pathway. siRNA-mediated downregulation of RA signaling resulted in significant upregulation of *LOXL1* and other genes involved in PEX-associated fibrosis. These data indicate an involvement of impaired RA signaling, downstream of thyroid hormone signaling, in PEX pathogenesis and suggest that the putatively causal intergenic variant rs7173049A>G could exert a protective effect by upregulating the expression of STRA6 in ocular tissues.

Results

Variant rs7173049 downstream of *LOXL1* shows no 'flipping' effect across populations

Deep sequencing of the entire *LOXL1* locus [chr15:74200000 to 74 260 000] in a total of 5570 PEX cases and 6279 controls from

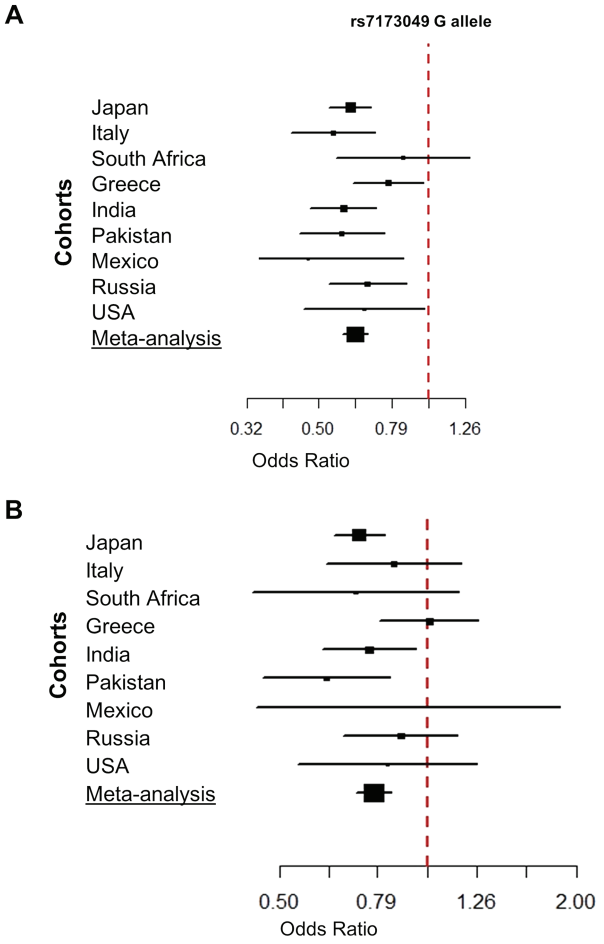

Figure 1. Forest plots for the association between rs7173049 and PEX syndrome in case–control cohorts from nine countries. (**A**) The effect of the rs7173049 G allele shows consistent odds ratios < 1 and is associated with decreased risk of PEX in all populations. (**B**) After adjustment for rs3825942, residual association of rs7173049 persists in the majority of cohorts. The horizontal lines denote the 95% confidence intervals of the odds ratio for each collection.

9 countries revealed a common non-coding sequence variant, rs7173049A>G, located 432 bp downstream of *LOXL1* stop codon and beyond the 3′UTR of *LOXL1*. This variant showed significant association with PEX syndrome and PEX glaucoma among different populations of Caucasian, Asian and African ancestry (OR = 0.63; $P = 4.27 \times 10^{-36}$; Table 1; Fig. 1A). We significantly replicated this association in an independent German cohort of 771 PEX patients and 1365 healthy subjects (OR = 0.59; $P = 7.42 \times 10^{-5}$; Table 1) using imputed genotype data (17). Conditioning for the canonical, most strongly associated 'flipped' variant rs3825942 (p.G153D) still resulted in a residual genome-wide significant association for rs7173049 (OR = 0.77; $P = 4.08 \times 10^{-10}$) with a consistent protective effect supported by minimal heterogeneity (I^2 index for heterogeneity, 19%; Table 1; Fig. 1B).

Thus, rs7173049A>G represents the first common variant at the broad *LOXL1* locus without allele effect reversal between populations of different ancestry, pointing to a potential biological significance of this locus.

Variant rs7173049 resides in an active regulatory region

Analysis of ENCODE project data (https://www.encodeproject.org) revealed that single nucleotide polymorphism (SNP) rs7173049 is located in a genomic region flanked by specific

Table 1. Association analysis for SNP rs7173049 in different populations; (**A**) Association results for rs7173049 obtained from *LOXL1* deep sequencing in 5570 PEX cases and 6279 controls, with rs7173049 G being strongly associated with decreased risk of PEX in nine different populations; (**B**) Replication of association in an independent German cohort of 771 PEX patients and 1365 healthy subjects using imputed genotype data

A

								Unconditioned analysis		Conditioned on LOXL1 rs3825942 (p.G153D)	
CHR	SNP	Position	Collection	Allele1	Freq. cases	Freq. controls	Allele2	P	OR	P	OR
15	rs7173049	74244610	Japan	G	0.2151	0.309	A	8.11×10^{-19}	0.61	8.63×10^{-8}	0.72
			Italy	G	0.155	0.2509	A	7.21×10^{-6}	0.5476	0.32	0.85
			South Africa	G	0.1947	0.222	A	0.4358	0.8475	0.17	0.71
			Greece	G	0.2568	0.3087	A	0.02156	0.7737	0.96	1.01
			India	G	0.3326	0.4602	A	3.01×10^{-7}	0.5844	0.014	0.76
			Pakistan	G	0.252	0.3683	A	4.98×10^{-5}	0.5778	0.0018	0.62
			Mexico	G	0.06048	0.1208	A	0.01163	0.4687	0.80	0.91
			Russia	G	0.1329	0.1846	A	0.001824	0.68	0.35	0.88
			USA	G	0.1486	0.2081	A	0.03387	0.6642	0.38	0.83
			Meta-analysis					**4.27×10^{-36} (Phet = 0.35)**	0.63 (I^2 = 10.7%)	**4.08×10^{-10} (Phet = 0.27)**	0.77 (I^2 = 19%)

B

CHR	SNP	Position	Collection	Allele1	Freq. cases	Freq. controls	Allele2	P	OR
15	rs7173049	74244610	Germany	G	0.1369	0.2101	A	7.42×10^{-5}	0.596

histone modifications (H3K27Ac), DNase I hypersensitivity sites and transcription factor binding sites marking active regulatory elements (Fig. 2A). To explore a potential regulatory activity of this site, dual luciferase reporter assays were performed by transiently transfecting disease-relevant cell types, i.e. human Tenon's capsule fibroblast (hTCF) and human trabecular meshwork cells (hTMCs), with pGL4.23 [*luc2*/minP] luciferase reporter plasmids containing a 200 bp DNA fragment surrounding rs7173049 with either allele A or G (rs717-A/G) upstream of a gene-unspecific minimal promoter. These reporter assays showed a significantly higher reporter activity for constructs containing both alleles of rs7173049 inserts compared to empty vector without the rs7173049 insert in hTCF (>8-fold; $P < 0.01$) and hTMC (>8-fold; $P < 0.05$) with the G alleles showing slightly higher effects than the A alleles in both cell types (Fig. 2B). This observation suggests an enhancer effect of this region with moderate allele-specific differences *in vitro*.

To further test an effect of the enhancer element on transcriptional activity of the *LOXL1* promoter, the 200 bp fragments with either rs7173049-A or -G allele (rs717-A/G) were cloned into pGL4.10 luciferase reporter plasmids upstream of the specific *LOXL1* core promoter (nucleotides −1438/+1) (23) and transiently transfected into hTCF and hTMC. In contrast to expectation, pGL4.10–*LOXL1* constructs did not show any statistically significant differences in reporter activity compared to control transfections with the basal *LOXL1* promoter construct without the rs7173049 insert (Fig. 2C). This observation indicates that the genomic region containing rs7173049 has no direct influence on *LOXL1* transcription but may regulate the transcriptional activity of neighboring genes other than *LOXL1*.

We also performed electrophoretic mobility shift assays (EMSAs) to determine specific DNA–protein interaction at rs7173049 genomic region. We used biotinylated 31 bp oligonucleotides containing allele A or G of rs7173049 and nuclear protein extracts from hTMC and hTCF. EMSAs yielded specific shifted bands with both extracts in a concentration-dependent manner (Fig. 2D, left). Shifts could be competitively inhibited by unlabeled oligonucleotides confirming sequence-specific interaction (Fig. 2D, right). Quantitative analysis of the shifted bands showed greater protein binding affinity to the sequence containing the protective allele G compared to that containing allele A ($P < 0.01$). The findings suggest a differential regulatory effect of rs7173049 genomic region on any genes nearby, which may be mediated by differential transcription factor binding.

Deletion of rs7173049 region enhances transcription of *STRA6* and *ISLR2*

Since regulatory elements can be located up to 1 Mb remote from the transcription unit (24), we sought to assess an effect of the enhancer element on all 31 genes contained within a region 1 Mb up- and downstream of rs7173049 (Fig. 3A). To this end, the CRISPR/Cas9 system was used to delete a 200 bp sequence around rs7173049 in HEK293T cells by a dual cut approach. In two separate experiments, HEK293T cells were transfected with two different pairs of guide RNAs (crRNA-F1/R1 and crRNA-F2/R2) by means of lipofection. For each experiment, four individual single cell-derived edited clones with a homozygous deletion of the target genomic region and six non-edited control clones were used for expression analysis of all 31 genes. As both experimental approaches yielded similar results, combined results of both probes are shown in Figure 3B. Quantitative real-time polymerase chain reaction (PCR) revealed a significant downregulation of *LOXL1* expression ($P < 0.05$) and significant upregulation of two genes downstream of rs7173049, i.e. *STRA6* ($P < 0.05$) and *ISLR2* ($P < 0.01$), in edited cells compared to non-edited control cells. Both genes were confirmed to be expressed in HEK293T cells at the protein level by immunofluorescence staining, reflecting the differences in mRNA expression levels seen after deletion of the rs7173049 region (Fig. 3C). The findings confirm a regulatory effect of rs7173049 genomic region *in vivo* and suggest an impact on transcriptional regulation of *LOXL1* and two neighboring genes, *STRA6* and *ISLR2*, which have not been previously related with PEX disease.

Verification of rs7173040–target genes relationships on tissue level

The *in vitro* data were further correlated with expression signatures of target genes in ocular tissues of PEX and control patients *in situ*. First, we evaluated whether the rs7173049 alleles correlated with expression levels of *LOXL1*, *STRA6* and *ISLR2* in ocular tissues ($n = 66$) independent of disease state. For that purpose, DNA samples of iris specimens isolated from 24 individuals with PEX syndrome and 42 individuals without PEX were used for genotyping of rs7173049, while mRNA expression levels were analyzed by quantitative real-time PCR. As shown in Figure 4A, iris tissue homozygous for the protective allele G showed significantly higher expression levels of *STRA6* (1.75-fold; $P < 0.05$) and *ISLR2* (2-fold; $P < 0.01$) compared to specimens harboring the A/A genotype. However, there was no significant correlation between rs7173049 alleles and expression levels of *LOXL1*, which suggests a direct regulatory effect on *STRA6* and *ISLR2* transcription only. When comparing their expression levels in PEX and control specimens, transcript levels of both *STRA6* and *ISLR2* were found to be significantly decreased in iris tissue derived from PEX patients compared to control samples ($P < 0.001$). Because *STRA6* and *ISLR2* have been previously reported to be highly expressed in the mouse retina (25,26), we included retinal tissue in our analysis. Again, transcript levels were significantly decreased in PEX specimens compared to age-matched controls ($P < 0.05$) (Fig. 4B).

At the protein level, STRA6, a cell surface receptor that regulates cellular uptake of vitamin A, was previously reported to be strongly expressed at blood–tissue barriers, such as the retinal pigment epithelium (RPE) of mouse eyes (26). Prominent staining of the RPE along its basolateral membranes could be confirmed in normal human eyes confirming specificity of the antibody (Fig. 4C, top left). STRA6 could be further immunolocalized to cell layers forming the blood–retinal and blood–aqueous barriers, i.e. endothelial cells of retinal (Fig. 4C, top center) and iridal blood vessels (BVs; Fig. 4C, middle left), the inner wall of Schlemm's canal (SC; not shown) and the pigmented ciliary epithelium (CE; Fig. 4C, bottom left). In corresponding tissues of PEX eyes, markedly reduced expression levels of STRA6 were observed, often in association with LOXL1-positive PEX material deposits (Fig. 4C).

ISLR2, a membrane protein required for axon growth during neural development, was previously demonstrated in the murine retina (25). In accordance with this report, ISLR2 predominantly localized to the retinal nerve fiber layer (NFL) and individual cells resembling astrocytes in the retinal ganglion cell (RGC) layer in normal human eyes (Fig. 4D, top left and center). In addition, prominent staining for ISLR2 could be observed along nerves traversing the corneal stroma (ST; not shown), in endothelial cells of iridal BVs (Fig. 4D, middle left and center) and in endothelial cells of the trabecular meshwork (TM) and SC

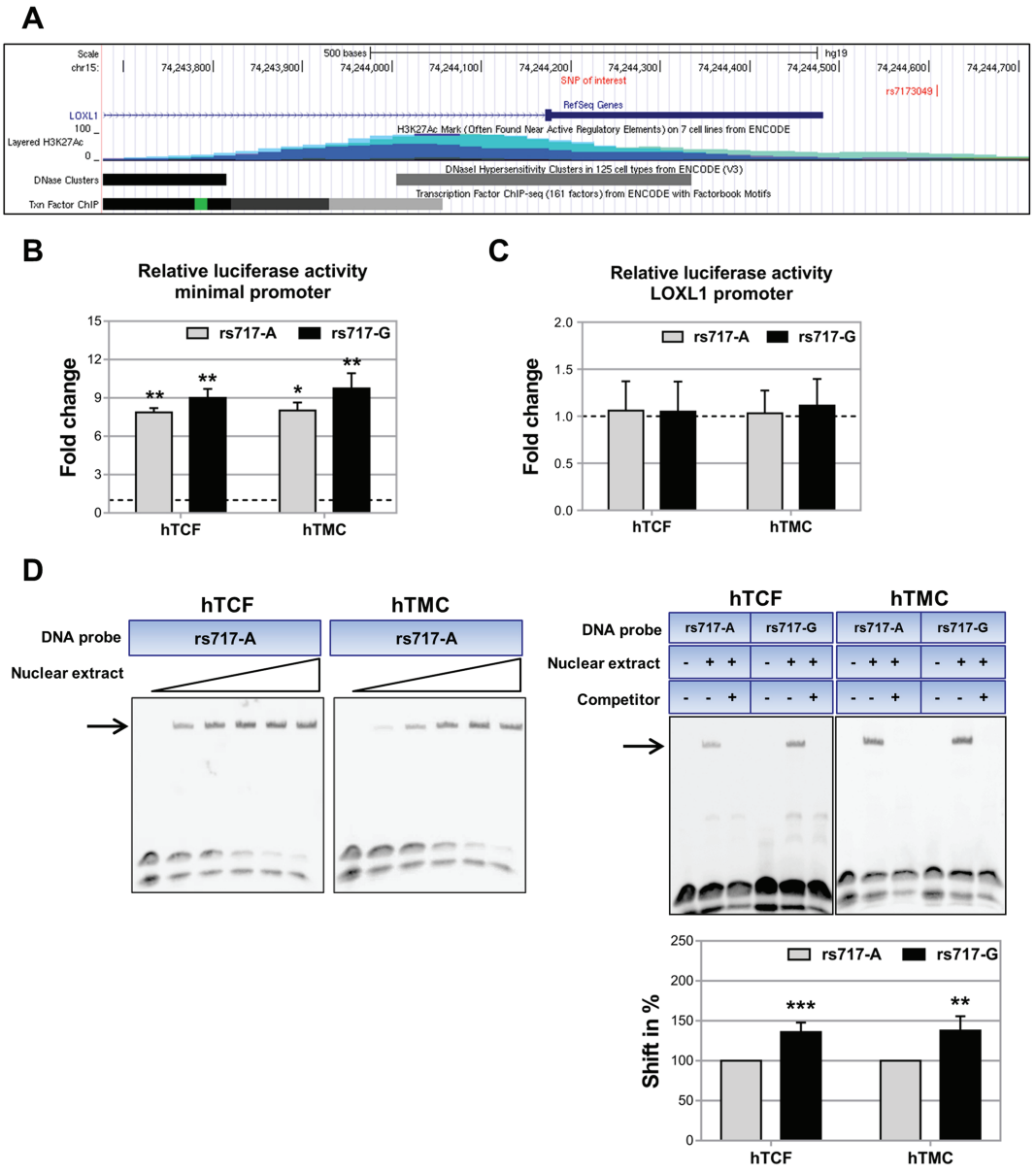

Figure 2. Location of SNP rs7173049 in an active regulatory genomic region. (**A**) Genomic region surrounding rs7173049 located downstream of *LOXL1* viewed in UCSC genome browser (http://genome.ucsc.edu: *GRCh37/hg19*). ENCODE Regulation Tracks specify layered histone marks for H3K27Ac, DNase hypersensitivity regions and transcription factor binding sites, which indicate active regulatory elements flanking the SNP of interest, rs7173049. (**B**) Dual luciferase reporter assays demonstrating significantly increased regulatory activity for pGL4.23 [*luc2*/minP] reporter constructs containing a 200 bp fragment surrounding rs7173049 with either allele A (rs717-A) or G (rs717-G) upstream of a gene-unspecific minimal promoter compared to pGL4.23 [*luc2*/minP] empty vector without the rs7173049 insert in hTCFs ($P < 0.01$) and TM cells (hTMC; $P < 0.05$). Results are expressed as the ratio of Firefly luciferase to Renilla luciferase and analyzed in relation to the transcriptional activity of the pGL4.23 empty vector set at 1 (dashed line). (**C**) Relative luciferase activity of pGL4.10-*LOXL1* reporter constructs containing a 200 bp fragment surrounding rs7173049 with either allele A (rs717-A) or G (rs717-G) upstream of the specific *LOXL1* core promoter was not increased over basal pGL4.10-*LOXL1* promoter activity without the rs7173049 insert in hTCF and hTMC. Results are expressed as the ratio of Firefly luciferase to Renilla luciferase and analyzed in relation to the transcriptional activity of the pGL4.10-*LOXL1* basal vector set at 1 (dashed line). (**D**) EMSAs using 31 bp biotinylated DNA probes containing rs7173049 A (rs717-A) or G (rs717-G) allele and nuclear extracts from hTCF and hTMC showing specific DNA–protein complexes (arrows). Following titration with increasing concentrations of nuclear proteins (left), shifted bands could be completely inhibited by unlabeled oligonucleotides proving specificity (right). Quantitative analysis of the shifted bands relative to the unshifted bands revealed allele-specific differences with significantly stronger binding of the G allele compared to the A allele set at 100%. Data represent mean values ± standard deviation (SD) of at least three independent experiments (*$P < 0.05$; **$P < 0.01$; ***$P < 0.001$).

wall (Fig. 4D, bottom left and center). In PEX tissues, markedly reduced expression levels of ISLR2 were observed (Fig. 4D).

Taken together, these results suggest that rs7173049 allele-dependent alterations in expression levels of STRA6 and ISLR2 could be involved in PEX pathogenesis. Notably, an involvement of STRA6 in PEX disease is further confirmed by additional genetic data; re-examination of an existing, previously published GWAS data set on a total of 9035 PEX cases and 17 008 controls from 24 countries, with respect to the discovery stage (18), revealed a single synonymous coding variant, rs11857410 (p.L111L), located in exon 5 of *STRA6* (NM_022369), showing a significant association with PEX ($P = 1.25 \times 10^{-5}$; OR = 1.16), but without reaching genome-wide significance. We replicated the association between rs11857410 and PEX in independent

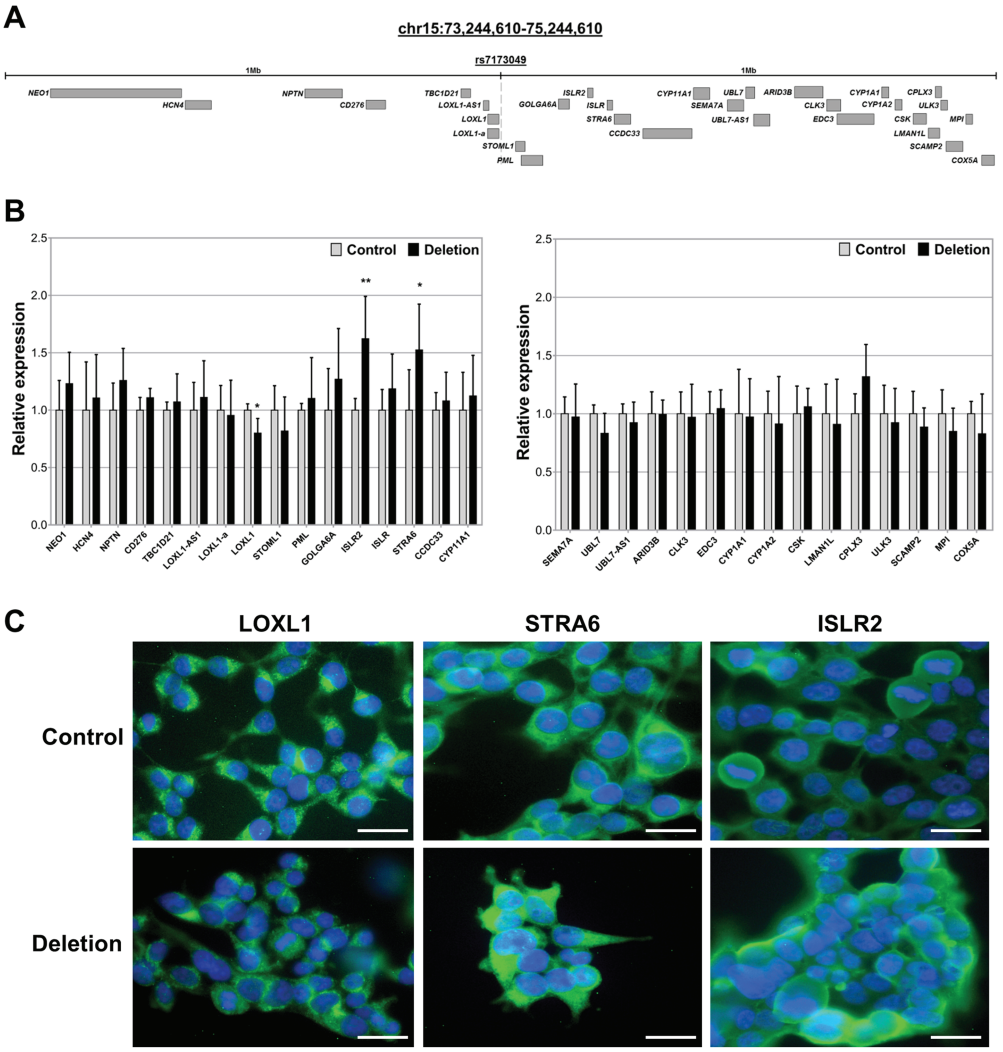

Figure 3. Transcriptional regulation of *LOXL1*, *STRA6* and *ISLR2* by genomic region containing rs7173049. (**A**) Schematic diagram showing the genomic region 1 Mb up- and downstream of rs7173049 (chr15:73244610-75244610) containing 31 genes. (**B**) Quantitative real-time PCR assays of all 31 neighboring genes showing significant downregulation of *LOXL1* as well as significant upregulation of *STRA6* and *ISLR2* in HEK293T cells after deletion of a 200 bp region flanking rs7173049 using CRISPR/Cas9 technology. Data represent mean values of eight edited (Deletion) and six non-edited (Control) clones; relative expression levels were normalized to *GAPDH* and are represented as means ± SD (*$P < 0.05$; **$P < 0.01$). (**C**) Immunofluorescence staining of HEK293T cells confirming reduced protein expression of LOXL1 as well as increased protein expression of STRA6 and ISLR2 in genome-edited cells compared to non-edited control cells. Nuclei are counterstained with DAPI (blue); scale bars are equal to 25 μM.

replication cohorts from Germany, Italy and India ($P = 0.00011$; OR = 1.26) in a total of 2151 PEX cases and 5798 controls (18). Altogether, these data amount to an association *P*-value of 1.2×10^{-8} (OR = 1.18) surpassing genome-wide significance. Further analysis of expression data from Genotype-Tissue Expression V7 project (https://gtexportal.org) revealed that SNP rs11857410 is located in an expression quantitative trait locus (eQTL) likely affecting *ISLR2* expression. In light of these and previous data showing that expression of *LOXL1* is regulated by RA (17,27), we further focused on the RA signaling pathway, which is activated by binding of the vitamin A-retinol binding protein 4 (RBP4) complex to STRA6 (28).

Dysregulation of RA receptor-mediated signaling in PEX tissues

We then analyzed expression levels of key components of the retinoid metabolic cascade up- and downstream of STRA6, i.e. RBP4, CRBP1 (cellular retinol-binding protein 1), CRABP2 (cellular RA-binding protein 2), RARα (RA receptor alpha) and RXRα (retinoid X receptor alpha), in ocular tissue, serum and aqueous humor samples from PEX patients and healthy controls. These proteins have central functions in retinol transport and cellular uptake, transformation into active RA and signal transduction of target genes in the nucleus (29). Significantly reduced mRNA expression levels of *CRBP1*, *CRABP2*, *RARA* and *RXRA* were observed in PEX tissue specimens ($n = 24$) compared to controls ($n = 42$; $P < 0.05$; Fig. 5A). Reduced expression levels of CRBP1, indicated by a specific band at 16 kDa, could also be confirmed at the protein level in iris (0.4-fold; $P < 0.001$) and ciliary body tissue (0.5-fold; $P < 0.01$) of PEX patients ($n = 4$) compared to controls ($n = 4$; Fig. 5B). The retinol carrier RBP4, indicated by a specific band at 23 kDa, was significantly reduced in serum (0.7-fold; $P < 0.05$) and aqueous humor (0.6-fold; $P < 0.01$) samples of PEX patients ($n = 8$) compared to age-matched controls ($n = 8$; Fig. 5C).

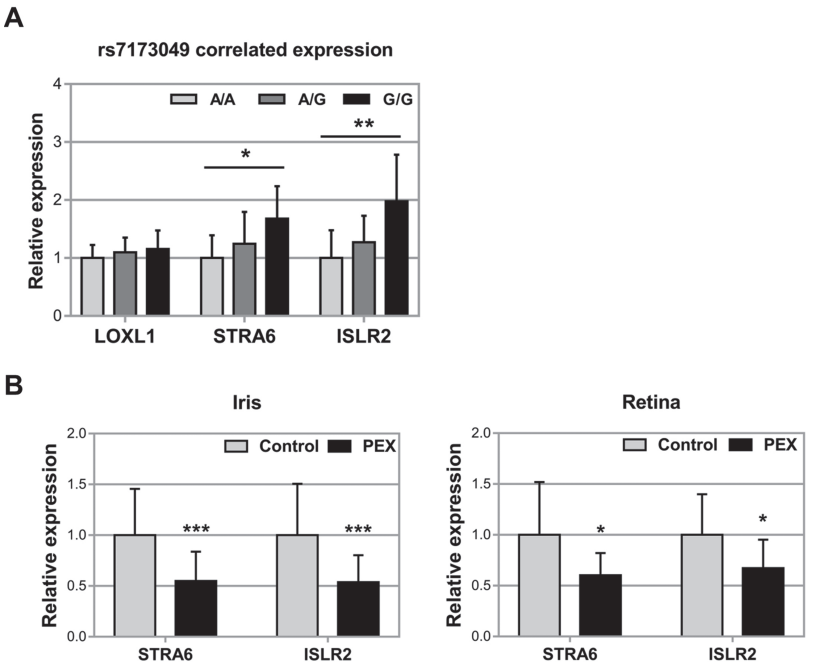

Figure 4. Correlation of rs7173049 genotype and tissue expression levels of STRA6 and ISLR2. (**A**) Genotype-correlated mRNA expression levels of *STRA6* and *ISLR2* in human iris tissue samples homozygous for allele A ($n = 33$) or allele G ($n = 5$) or heterozygous for both alleles ($n = 28$) at rs7173049 using real-time PCR technology. Expression levels of *STRA6* and *ISLR2* are significantly increased in specimens homozygous for the protective allele G compared to samples with A/G and A/A genotype. (**B**) Expression of *STRA6* and *ISLR2* mRNA in ocular tissues (iris and retina) derived from normal human donors (control, $n = 42$) and donors with PEX syndrome ($n = 24$) using real-time PCR technology. Expression levels were significantly reduced in PEX specimens compared to control specimens. The relative expression levels were normalized relative to GAPDH and are represented as mean values ± SD ($^{*}P < 0.05$; $^{**}P < 0.01$; $^{***}P < 0.001$). (**C**) Expression of STRA6 protein in ocular tissues (retina, iris and ciliary body) of normal human donor eyes and donor eyes with PEX syndrome, as determined by immunofluorescence labeling. In normal eye tissues (control), STRA6 immunopositivity (green fluorescence) is observed in the RPE overlying the choroid (CH), retinal BVs (asterisk) within the RGC layer, iridal BVs (asterisk) in the iris ST and the inner layer of the CE adjacent to the ciliary ST. Expression levels are reduced in tissues of PEX eyes, and reduced staining intensities are often associated with LOXL1-positive PEX material accumulations (PEX, red immunofluorescence) in iris blood vessel walls and on the surface of the CE. (**D**) Expression of ISLR2 protein in ocular tissues (retina, iris and TM) of normal human donor eyes and donor eyes with PEX syndrome, as determined by immunofluorescence labeling. In normal control tissues, ISLR2 immunopositivity (green fluorescence) is observed in the retinal NFL, single cells (arrow) of the retinal ganglion cell layer (RGC) adjacent to BVs (asterisk), endothelial cells of BVs (asterisks) in the iris ST, and endothelial cells of the TM and SC. Markedly reduced staining intensities were seen in tissues of PEX eyes (INL means inner nuclear layer; ONL, outer nuclear layer; DAPI nuclear counterstain in blue).

Inhibition of RA signaling by siRNA-mediated knockdown of *RXRA* in hTCF and hTMC resulted in a significant upregulation of PEX-relevant genes, including *LOXL1*, *ELN*, *FBN1* (*fibrillin-1*) and *TGFB1* (*transforming growth factor beta 1*), compared to scramble siRNA-transfected control cells ($P < 0.01$; Fig. 5D). In contrast, stimulation of RA signaling by addition of 2.5 μM RA upregulated expression levels of *RXRA* and downregulated expression levels of *LOXL1*, *ELN*, *FBN1* and *TGFB1* ($P < 0.05$; Fig. 5E). These results suggest that diminished RA receptor-mediated signaling in PEX cells and tissues may be involved in transcriptional upregulation of PEX-relevant genes and may drive fibrosis in PEX pathogenesis.

Potential mechanisms of target gene regulation

To finally identify the molecular mechanisms by which sequence variation at rs7173049 may modulate *STRA6* and *ISLR2* gene regulation, we performed *in silico* analysis using the PROMO bioinformatics program to identify putative transcription factor binding sites potentially affected by rs7173049 polymorphism. We detected a total of five transcription factors predicted to bind to the chromosomal region flanking SNP rs7173049 (±15 bp), i.e. c-Jun (T00133),glucocorticoid receptor alpha (GR-alpha; T00337), estrogen receptor alpha (ER-alpha; T00261), X-box binding protein 1 (XBP-1; T00902) and Yin Yang 1 (YY1; T00915), but only one transcription factor, THRβ1 (T3R-beta1; T00851), was affected by sequence variant differences between allele A and allele G of rs7173049 (Fig. 6A). In fact, T3R-beta1 is predicted to bind exclusively to the DNA sequence containing the protective allele G and was, therefore, selected for further analysis. Supershift assays using a biotinylated 31 bp oligonucleotide containing allele G of rs7173049, nuclear protein extracts of hTCF and an antibody against thyroid hormone receptor alpha and beta (THRα/β) confirmed specific binding by disruption of protein–DNA complexes and generation of supershifted bands (Fig. 6B). However, antibodies against any potential heterodimeric binding partners of THR, i.e. RXRα,β,γ and RAR α,β,γ (30), failed to show any specific binding to the DNA probe. Comparison of sequences containing the A allele (rs717-A) and the protective G allele (rs717-G) of rs7173049 in (super)shift experiments with anti-THRα/β antibody revealed distinct shifted and supershifted bands for the rs717-G probe, which were largely absent when the rs717-A probe was used (Fig. 6C). Bands which were competitively inhibited by unlabeled oligonucleotides were considered to reflect sequence-specific interactions. Specific binding of human recombinant THRβ protein to the rs717-G probe was used as positive control and resulted in two shifted bands presumably representing THR monomers and homodimers (Fig. 6D) (30). Finally, siRNA-mediated knockdown of *THRB* in hTCF resulted in downregulation of key components of the RA signaling pathway, including *STRA6*, *CRBP1*, *CRABP2*, *RARA* and *RXRA*, compared to scramble siRNA-transfected control cells (Fig. 6E).

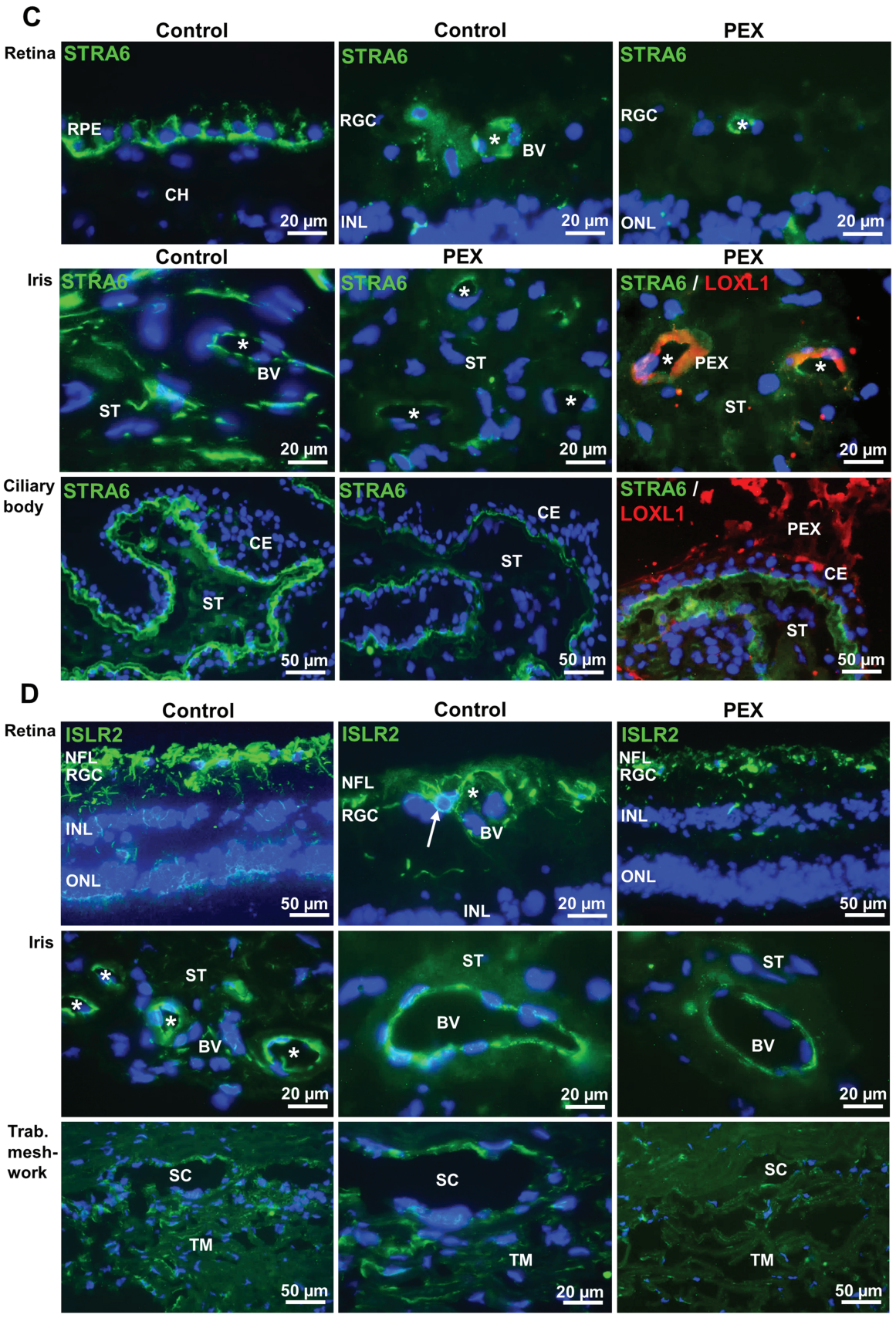

Figure 4. Continued

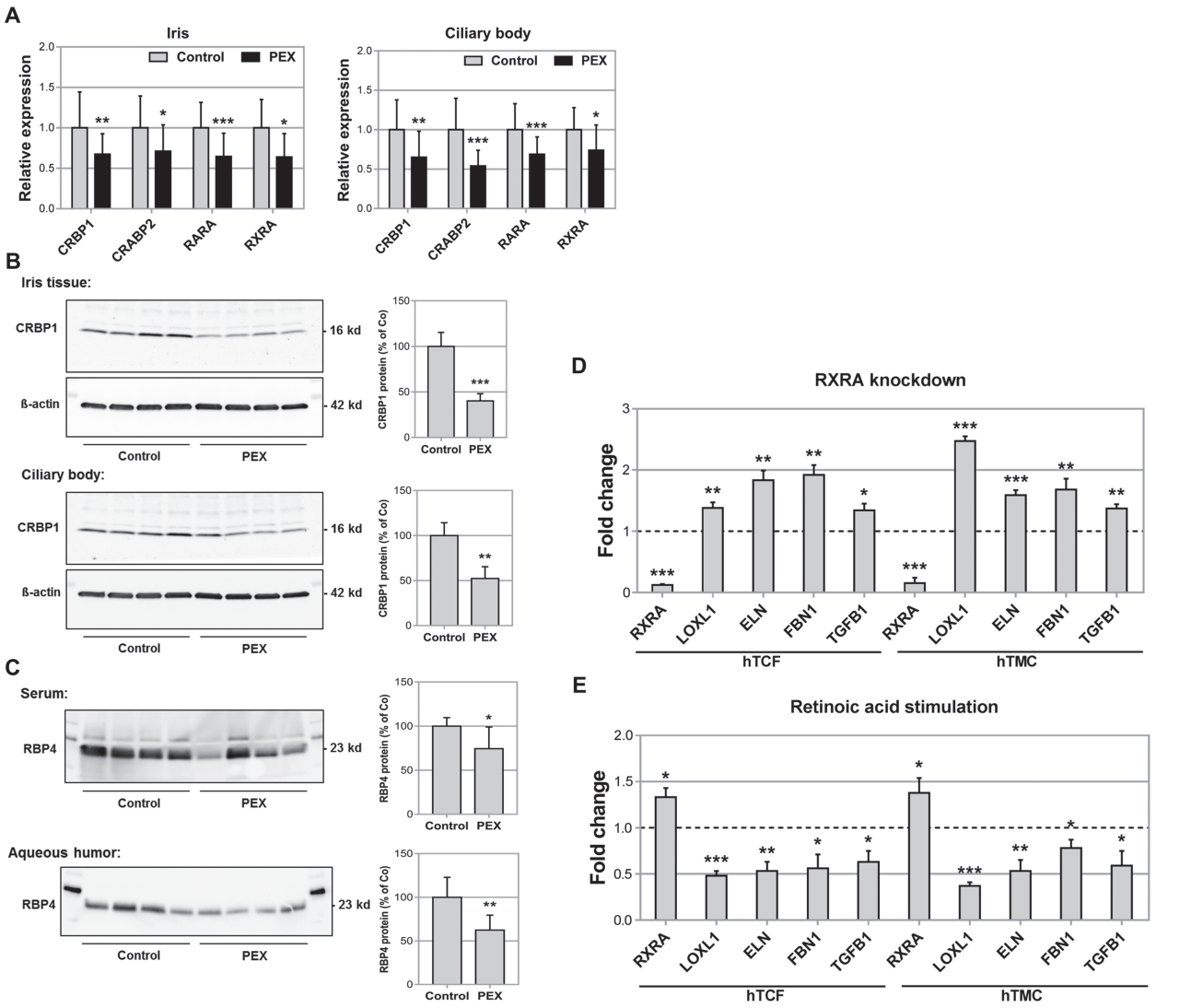

Figure 5. *Diminished RA signaling in PEX tissues.* (**A**) Expression of *CRBP1*, *CRABP2*, *RARA* and *RXRA* mRNA in iris ($n = 42$) and ciliary body specimens ($n = 22$) from normal human donors (control) and donors with PEX syndrome ($n = 24$) using real-time PCR technology. Expression levels were significantly reduced in PEX specimens compared to control specimens. The relative expression levels were normalized relative to *GAPDH* and are represented as mean values ± SD. (**B**) Western blot analysis of CRBP1 protein expression in iris and ciliary body tissue from normal donors (control, $n = 4$) and patients with PEX syndrome ($n = 4$). Protein expression is normalized to the house-keeping gene ß-actin and is expressed as percent of the expression in controls. (**C**) Western blot analysis of RBP4 protein in serum and aqueous humor samples from cataract patients (control, $n = 4$) and patients with PEX syndrome ($n = 4$). RBP4 protein is normalized to total protein content and is expressed as percent of controls (data represent mean values ± SD of eight samples; $^{*}P < 0.05$; $^{**}P < 0.01$ $^{***}P < 0.001$). (**D**) Real-time PCR analysis of *RXRA*, *LOXL1*, *ELN*, *FBN1* and *TGFB1* mRNA in hTCFs ($n = 4$) and TM cells (hTMC, $n = 4$) transfected with *RXRA*-specific siRNA or scrambled control siRNA; expression levels were normalized relative to *GAPDH* and expressed relative to mock-transfected controls (dashed line; $^{*}P < 0.05$; $^{**}P < 0.01$; $^{***}P < 0.001$). (**E**) Real-time PCR analysis of *RXRA*, *LOXL1*, *ELN*, *FBN1* and *TGFB1* mRNA in hTCF and hTMC without and with stimulation by 2.5 μM RA for 48 h; expression levels were normalized relative to *GAPDH* and expressed relative to unstimulated controls (dashed line; $^{*}P < 0.05$; $^{**}P < 0.001$; $^{***}P < 0.0001$).

These data suggest that the molecular mechanisms by which sequence variation at rs7173049 can modulate *STRA6* gene regulation are mediated by differential effects of THRβ, showing specific binding to the protective allele G of rs7173049. This functional mechanism may be also involved in reduced expression of *STRA6* and downstream components of RA signaling in risk allele carriers and PEX patients.

Discussion

According to well-powered genetic association studies and meta-analyses, *LOXL1* is the predominant genetic risk factor for PEX syndrome/glaucoma showing uniformly large genetic effect sizes with odds ratios up to 20-fold in all populations throughout the world (10,13,18). However, to date, all PEX-associated common risk variants have been confuted any causality due to allele effect reversal in populations of different ancestry (10,17,18). Since causal variants for complex diseases may lie outside coding regions of protein-coding genes (31,32), we refined and extended our search for common variants to intergenic regions within the broad *LOXL1* locus.

Our resequencing effort revealed one common non-coding sequence variant, rs7173049A>G, downstream of *LOXL1*, which was significantly associated with PEX across different populations around the world, with the minor allele G being consistently enriched in controls without any flipped allele effect. This

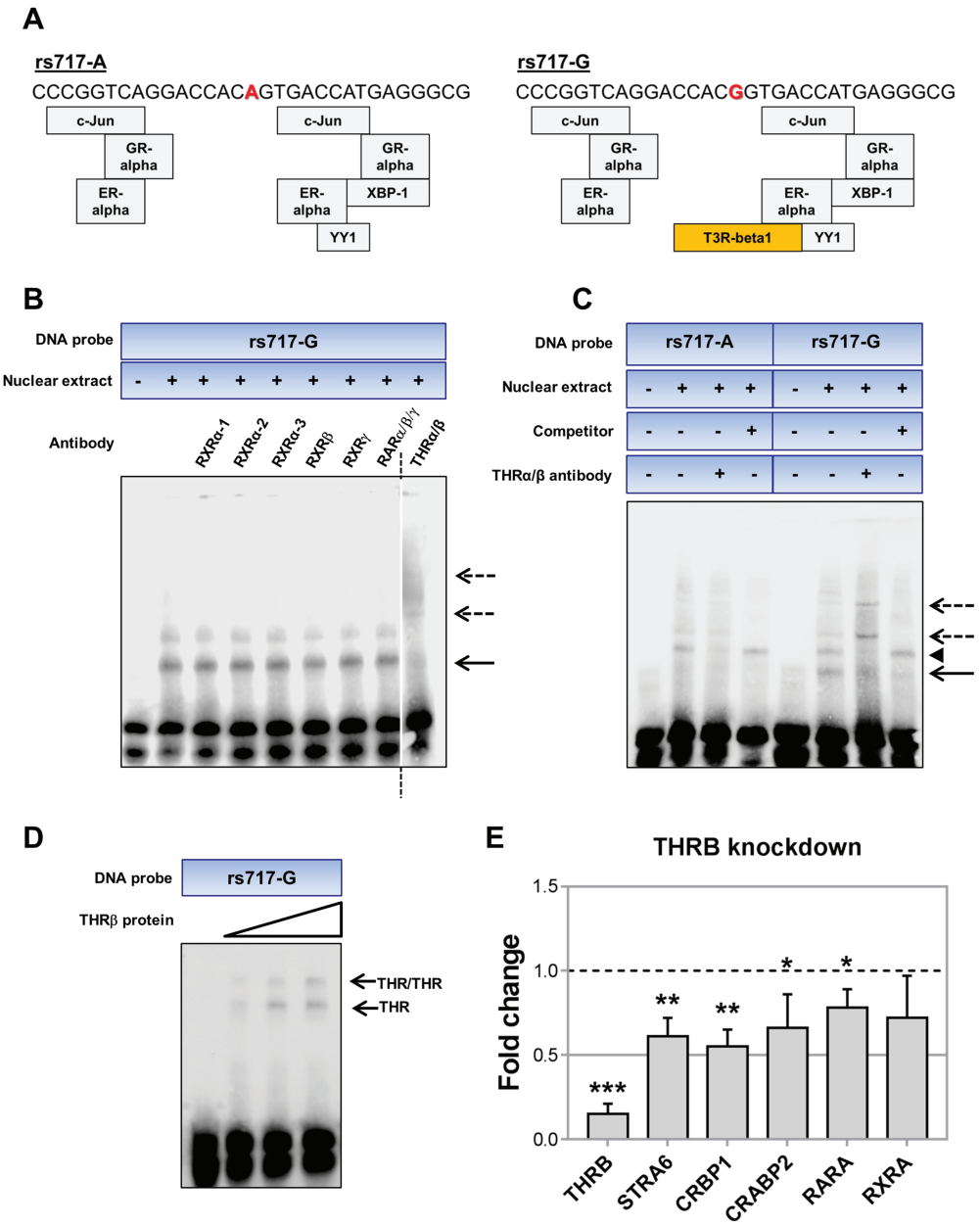

Figure 6. Allele-specific transcription factor binding at the genomic region surrounding rs7173049.**(A)**Transcription factor binding sites overlapping SNP rs7173049 (marked in red) regions (±15 bp) as predicted by the PROMO bioinformatics program. Differential binding to sequences containing the protective G allele (rs717-G) compared to sequences containing the A allele (rs717-A) was only predicted for T3R-beta1 (THRβ1). Each gray/orange box indicates one transcription factor: GR-alpha, ER-alpha, XBP-1 and YY1. **(B)** Supershift assays with 31 bp biotinylated DNA probes containing rs7173049 G allele (rs717-G), nuclear extracts from hTCFs and specific antibodies against candidate transcription factors RXRα-1,2,3, beta (RXRβ) and gamma (RXRγ), RARα/β/γ and thyroid hormone receptor alpha/beta (THRα/β) showing disruption of the shifted DNA–protein complex (solid arrow) and formation of supershifted bands (dotted arrows) with the THRα/βantibody. Dotted black line indicates a cut and junction of two parts of the same membrane. **(C)** Supershift assays with THRα/β antibody attenuated the shifted DNA–protein complex (solid arrow) and produced distinct supershifted bands (dotted arrows) with DNA probes containing the protective allele G of rs7173049 (rs717-G). No supershifted bands were detected with probes containing the A allele (rs717-A). Bands which were not competitively inhibited by unlabeled oligonucleotides (arrowhead) were considered unspecific. **(D)** Increasing amounts of recombinant THRβ protein were used in positive control experiments to show a specific interaction with the DNA probe containing the protective G allele of rs7173049 (rs717-G). DNA–protein complexes (arrows) presumably represent thyroid hormone receptor (THR) monomers and homodimers. **(E)** Real-time PCR analysis of *THRB*, *CRBP1*, *CRABP2*, *RARA* and *RXRA* mRNA in hTCFs ($n = 4$) transfected with *THRB*-specific siRNA or scrambled control siRNA; expression levels were normalized relative to *GAPDH* and expressed relative to mock-transfected controls (dashed line; ($^{*}P < 0.05$; $^{**}P < 0.01$ $^{***}P < 0.001$).

variant was not considered in our previous study (18) because of its location outside the intragenic region of *LOXL1*. We did not identify any other variant at *LOXL1* in strong LD (defined as pairwise $r^2 > 0.7$) with rs7173049. All other associated common variants at the *LOXL1* locus (17,18) showed allele reversal in one or more ethnic groups and therefore did not surpass genome-wide significance, when meta-analysis using the inverse-variance, random effects method was applied ($P > 1 \times 10^{-5}$). These

findings suggested that the identified rs7173049 variant may represent a plausible candidate for a true causal relationship with the PEX phenotype.

We then provided experimental evidence for a functional enhancer-like effect of the genomic region surrounding rs7173049, supported by luciferase reporter assays and differential protein binding at the polymorphic site *in vitro*. Even though we could not show any direct effect on *LOXL1* promoter activity, we observed a moderate indirect effect on *LOXL1* regulation after CRISPR/Cas9 deletion of the genomic region, which may be mediated by a yet unknown intermediary factor. However, a more pronounced *cis*-regulatory effect was seen on the expression of two distant genes, *STRA6* and *ISLR2*, 227 and 177 kb downstream of rs7173049, respectively. Since enhancer and repressor elements can act over long distances from their target genes (33) through DNA looping facilitated by transcription factor binding, and since *LOXL1* alone cannot explain the complex pathophysiology of PEX syndrome (18), we analyzed the regulation of the two novel genes and their putative role in PEX pathophysiology. Whereas the rs7173049 alleles did not correlate with LOXL1 tissue expression levels, we found that the protective G allele of rs7173049 correlates with increased tissue expression levels of *STRA6* and *ISLR2*, which both were significantly reduced in PEX tissues compared to age-matched controls. We then specifically focused on the role of *STRA6*, because lysyl oxidases are known to be regulated by RA (17,34), and because re-examination of published GWAS data (18) revealed a hitherto unreported synonymous coding variant at *STRA6*, rs11857410, which was associated with PEX on a genome-wide level after inclusion of additional cohorts.

STRA6 is a cell surface receptor that transports diet-derived vitamin A or retinol, which circulates in the blood in a protein complex containing RBP4 and transthyretin, into target cells (28,35,36). Subsequent conversion of retinol into retinaldehyde (retinal) and RA is supported by cellular binding proteins, such as CRBPs and CRABPs, and two enzyme families, the alcohol or retinol dehydrogenases (ADHs/RDHs) and the aldehyde dehydrogenases (ALDHs) (37). RA, the main active metabolite of vitamin A, binds to nuclear receptors, RAR and RXR, to regulate gene transcription by binding to RA response elements in diverse target genes. In addition to serving as a retinol transporter, STRA6 is a ligand-activated signaling receptor that activates JAK/STAT signaling and downstream induction of STAT-target genes (38).

STRA6 exhibits complex expression patterns during development and homeostasis, probably indicating tissues to which retinol is preferentially delivered (26). Thus, STRA6 is highly expressed in epithelia of blood–tissue barriers, such as the RPE and the choroid (CH) plexus of the brain, and is transcriptionally upregulated by RA (39). Mouse and zebrafish models have highlighted the importance of STRA6 for vitamin A uptake and homeostasis in ocular tissues (36,40). Interestingly, *STRA6* mutations constitute the only demonstrated cases of human mutations that affect a gene from the retinoid pathway and lead to a complex spectrum of developmental abnormalities including micro/anophthalmia, heart defects, pulmonary dysplasia and diaphragmatic hernia (41,42). A similar disease spectrum, including relative anterior microphthalmos, atrial fibrillation, obstructive pulmonary disease and inguinal hernias, has been reported to occur in PEX patients (9,43,44). Silencing of *STRA6* can also cause tissue fibrosis via suppression of STRA6 cascades through upregulation and activation of TGF-ß1 and collagen type I (45).

The RA pathway displays pleiotropic and vital functions which are essential for eye development and eye function, particularly vision, throughout life (46,47). Dysregulated RA signaling and decreased availability of RA can contribute to a spectrum of developmental ocular disorders, such as primary congenital glaucoma (48), and has also been associated with age-related ocular and systemic diseases, including primary open-angle glaucoma, age-related macular degeneration and neurodegenerative disorders such as Alzheimer disease (49–51). For instance, Alzheimer patients have lower serum concentrations of vitamin A accompanied by defective RA transport and function in the brain (49,52). Vitamin A-deficient mice accumulated amyloid-ß peptides, whereas the formation of amyloid-ß fibrils could be inhibited by administration of RA *in vitro* and *in vivo* resulting in neuroprotective effects (53, 54). The underlying molecular mechanisms appear to involve modulation of NFκB signaling, activation of α-secretase and inhibition of γ-secretase-mediated cleavage of amyloid precursor protein (55–57).

RA signaling has also received considerable attention in the pathobiology of fibrosis (58,59). Although the reported effects of RA on matrix production and fibrosis development are controversial (60), the majority of studies found that RA administration attenuated or even prevented experimental fibrosis in multiple organ systems by suppressing expression of matrix proteins, such as collagens, laminin and fibronectin, via context-dependent downregulation of TGF-ß, IL-6, PI3K-Akt, NFκB and Wnt/ß-catenin signaling (61–65). Conversely, vitamin A deficiency and diminished RA signaling have been linked to fibroblast activation, upregulation of matrix production and fibrosis via activation of TGF-ß expression and signaling (66,67). In fact, the structure and composition of the extracellular compartment are known to become profoundly altered as a result of vitamin A deficiency (68).

Based on the pertinent literature and the evidence provided by this study, it is suggested that vitamin A deficiency and diminished RA signaling may also be involved in the pathobiology of abnormal matrix deposition characterizing PEX syndrome. Levels of RBP4, which mediates retinol transport in body fluids, were significantly lower in serum and aqueous humor samples from PEX patients than those from control subjects. Expression levels of STRA6, which mediates the rate-limiting transport of retinol into target cells, together with key components of the retinoid metabolic cascade downstream of STRA6 were significantly reduced in ocular tissues of PEX patients compared to age-matched controls. On the protein level, expression of STRA6 was mainly observed in cells forming blood–ocular barriers, including the RPE and retinal BV endothelia forming the blood-retina barrier, and the epithelium of the ciliary body and endothelia of iridal BVs and SC, forming the blood–aqueous barrier (69,70). Notably, all anterior segment tissues expressing STRA6 are known to be involved in the fibrotic PEX process showing accumulation of abnormal fibrillar aggregates on their surfaces. Accordingly, reduced labeling for STRA6 in respective tissues of PEX patients was spatially associated with accumulation of LOXL1-positive PEX material deposits. Thus, it is tempting to speculate that decreased RA signaling may promote excessive matrix production and cross-linking in PEX-associated fibrosis, a notion that is also supported by upregulation of LOXL1, TGF-β1, ELN and FBN1, which constitute major components of PEX deposits, after siRNA-mediated downregulation of RA signaling in PEX-relevant cell lines. However, the functional mechanisms by which impaired RA signaling causes tissue fibrosis still remain to be analyzed.

The functional molecular mechanisms by which rs7173049 polymorphism influences *STRA6* expression appears to involve differential, allele-dependent binding of the transcription factor

THRβ. THRs belong to the nuclear hormone receptor superfamily and act as ligand-dependent transcription factors mediating the biological effects of thyroid hormone (71). Two distinct genes, *THRA* and *THRB*, encode several receptor isoforms, predominantly THRα1 and THRβ1, which are expressed in different tissues and exhibit distinctive functional roles. THRs exert their effects on gene expression through direct interaction with specific DNA sequences known as thyroid hormone response elements, related to the sequence (G/A)GGT(C/G)A, either as monomers, homodimers or heterodimers (30,72). In the absence of ligand, THRs can act as repressors or activators of transcription, dependent on the presence of co-regulatory proteins. Several genes involved in retinoid metabolism, such as *RXRA* and *ALDH1A1/A3* (*aldehyde dehydrogenase 1 family members A1, A3*), are among the direct target genes regulated by thyroid hormone, suggesting that thyroid hormone signaling lies upstream of RA signaling in the brain (73–75). Based on allele-specific binding of THRβ to the protective rs7173049-G allele, corresponding to the presence of the hormone response element sequence GGTGA and downregulation of key components of the RA pathway following *THRB* knockdown, we suggest that interaction of thyroid hormone and RA signaling may be also important in the pathogenesis of PEX syndrome.

In addition to *STRA6*, deletion of the locus surrounding rs7173049 led to upregulation of *ISLR2*, a membrane protein which reveals highest expression levels in the brain and in the retina of mice (25). ISLR2 plays a role in the development of the nervous system and optic tract (76) but remains poorly characterized, particularly in humans. Based on its prominent expression pattern in the retinal NFL, as shown in this study, reduced expression levels of ISLR2 in the retina of PEX eyes may be involved in glaucoma development in PEX patients. Interestingly, the PEX-associated, synonymous coding variant at *STRA6*, rs11857410, has been indicated as a potential eQTL for ISLR2 regulation in neuronal tissues (www.gtexportal.org/). In line with this, transcript levels of *ISLR2* could be induced by RA stimulation (>3-fold; $P < 0.05$) in PEX-relevant cell types (data not shown). However, the potential interaction between RA receptor-mediated signaling and ISLR2 regulation as well as the role of ISLR2 in PEX pathogenesis remain to be clarified.

In summary, these findings indicate a statistically significant and consistent association between the G allele of the intergenic variant rs7173049A>G downstream of *LOXL1* and decreased risk of PEX syndrome/glaucoma in different ethnic populations, pointing to a biological and clinical significance in disease pathogenesis. The protective effects may be mediated by upregulation of STRA6, downstream of thyroid hormone signaling, in ocular tissues at blood barriers and by upregulation of ISLR2 in the retina. The genotype–phenotype correlation analysis led to the discovery of an involvement of the RA signaling pathway in the complex pathogenesis of PEX syndrome/glaucoma, further corroborated by a newly identified genome-wide significant association of PEX with a synonymous coding variant at *STRA6*, which also potentially affects protein expression and function (77). In view of the known environmental risk factors for PEX syndrome/glaucoma including UV radiation (11), retinoid metabolism in PEX tissue may be influenced not only by genetic but also by environmental and dietary factors (78) requiring further studies.

Limitations of this study are that rs7173049 association cannot explain the flipped allele phenomenon observed for all common variants in intragenic regions of *LOXL1*, and that its significance for *LOXL1* regulation remains unclear. Although *LOXL1* was not directly influenced by rs7173049 polymorphism, alterations in retinoid metabolism may indirectly influence LOXL1 expression levels. We recently identified *LOXL1* as target for RXRα binding regulating *LOXL1* transcription (17). Here, we further demonstrate an influence of RA signaling on expression of *LOXL1* and its extracellular substrates ELN and fibrillin, which represent integral components of the stably cross-linked fibrillar aggregates accumulating in tissues of PEX patients (79). Although the molecular mechanisms underlying increased matrix production and fibrosis are not yet clear, the RA receptor pathway may be a candidate for therapeutic intervention and can be potentially targeted to treat fibrotic alterations caused by insufficient tissue retinoid levels in PEX patients (80).

Materials and Methods

Patient collection and study approval

This study utilized nine case–control data sets from Japanese, Italian South African, Greek, Indian, Pakistan, Mexican, Russian, American and German cohorts (18). DNA and tissues from all patients with PEX syndrome or PEX glaucoma and from control subjects without PEX were obtained after informed written consent from each participant and used in accordance with the principles of the Declaration of Helsinki for experiments involving human tissues and samples. All study sites obtained ethics approval from their respective institutional review board or ethics committee.

LOXL1 targeted resequencing, genotyping and association analysis

Deep sequencing of the *LOXL1* locus (exons, introns, 5′ and 3′ flanking regions; spanning coordinates chr15:74200000 to 74260000) was performed on a total of 5570 PEX cases and 6279 controls from Japan (2827 cases and 3013 controls), Greece (355 cases and 1075 controls), Italy (454 cases and 267 controls), Russia (476 cases and 859 controls), United States (212 cases and 161 controls), Mexico (116 cases and 205 controls), South Africa (95 cases and 250 controls), India (648 cases and 263 controls) and Pakistan (383 cases and 186 controls) as previously described (18). We captured the entire *LOXL1* genomic region (both coding and non-coding) using the Roche NimbleGen SeqCap (Roche NimbleGen Inc., Madison, WI) easy probe kit. PEX cases and controls were captured together to minimize differential batch effects between kits. Raw sequence reads were processed from the beginning by aggregating binary alignment map (BAM) files from unaligned sequence reads using PICARD (https://broadinstitute.github.io/picard/), BWA (81) and GATK (https://software.broadinstitute.org/gatk/best-practices/) software packages following best practice guidelines. We excluded all duplicate reads from further analysis. Genetic variants were identified and called (genotyped) from recalibrated BAM files using the Haplotype caller function within the GATK software package. The capture chemistry and bioinformatics methods have previously been described (82,83). We only included high quality variants for statistical analysis by applying strict filters, such as allelic balance > 20% or <80%, genotype quality >25, as well as depth >10×. In addition, each variant must have had an overall genotyping success rate of > 95%, minor allele frequency >1% and a genotype distribution not significantly violating Hardy–Weinberg equilibrium ($P > 1 \times 10^{-5}$ for deviation).

Affymetrix genotype data from 771 PEX patients and 1365 control individuals from an independent population-based case–control study from Germany (17) were imputed into the

1000 Genomes phase 3 data set (84) using IMPUTE2 (85). We only included high-quality imputed variants with info score >0.9 and genotyping completion rate >0.95. A score-based logistic regression was performed using SNPTEST2 with age and gender as covariates for association analysis of SNP rs7173049 as previously reported (17). Logistic regression, as implemented in PLINK, was used to perform conditional analysis. Cochran's Q test and accompanying I^2 index was performed to calculate heterogeneity index (18). Forest plots were drawn using R statistical software package.

Association for the *STRA6* variant rs11857410 in replication cohorts from Germany (741 cases and 1325 controls), Italy (474 cases and 1511 controls) and India (936 cases and 2962 controls) (18) was calculated using logistic regression, and meta-analysis of replication collections was performed using inverse-variance weighted, fixed effects meta-analysis.

Human tissues

Human donor eyes used for corneal transplantation with appropriate research consent were obtained from donors of European origin and processed within 20 h after death. Informed consent to tissue donation was obtained from the donors or their relatives, and the protocol of the study was approved by the Ethics Committee of the Medical Faculty of the Friedrich-Alexander-Universität Erlangen-Nürnberg (no. 4218-CH) and adhered to the tenets of the Declaration of Helsinki for experiments involving human tissues and samples.

For RNA and DNA extractions, 24 donor eyes with manifest PEX syndrome (mean age, 77 ± 8 years) and 42 normal appearing age-matched control eyes without any known ocular disease (mean age, 72 ± 9 years) were used. For protein extractions, four donor eyes with manifest PEX syndrome (mean age, 73 ± 9 years) and four normal appearing age-matched control eyes without any known ocular disease (mean age, 76 ± 8 years) were used. For immunohistochemistry, ocular tissues were obtained from five donor eyes with PEX syndrome (mean age, 73 ± 8 years) and five control eyes (mean age, 70 ± 6 years). The presence of characteristic PEX material deposits in manifest disease was assessed by macroscopic inspection of anterior segment structures and confirmed by electron microscopic analysis of small tissue sectors. Ocular tissues were prepared under a dissecting microscope and shock frozen in liquid nitrogen. Aqueous humor (aspirated during cataract or filtration surgery) and serum samples were collected from eight patients with cataract (mean age, 73.6 ± 6 years) and eight patients with manifest PEX syndrome (mean age, 79 ± 8 years), immediately frozen in liquid nitrogen and stored at −80°C. All individuals underwent routine ophthalmologic examination for clinical signs of PEX syndrome after pupillary dilation.

TaqMan SNP Genotyping Assay was used to genotype DNA extracted from ocular tissues for SNP rs7173049 (C_28958055_10; Applied Biosystems, Foster City, CA). TaqMan assays were confirmed by Sanger sequencing.

Cell culture

Tenon's capsule biopsies were obtained from six patients (mean age, 12 ± 4 years) during strabismus surgery. Primary hTCF cultures were established as previously described (86) and maintained in Dulbecco's Modified Eagle's Medium (DMEM/Ham's F12; Invitrogen, Darmstadt, Germany) containing 15% (v/v) fetal bovine serum (FBS) and 1% antibiotic–antimycotic solution (PSA; Invitrogen). Primary hTMC from three different donors were obtained from Provitro (Berlin, Germany) and grown in DMEM supplemented with 10% FBS and 1% PSA. Both hTCF ($n = 4$) and hTMC ($n = 4$) were stimulated with 2.5 μM RA (Sigma-Aldrich, Munich, Germany) under serum-free conditions for 48 h as previously described (27). The human embryonic kidney cell line HEK293T was obtained from ATCC (Manassas, VA) and grown in DMEM (with 4.5 g/l glucose) supplemented with 10% FBS and 1% PSA. For immunofluorescence staining, HEK293T cells were seeded in 2-well chamber slides at a density of 3×10^5 cells/well and maintained for 24 h. All cells were maintained at 37°C in a humidified 95% air–5% CO_2 atmosphere.

Plasmid construction and dual luciferase reporter assay

Two different reporter vectors, the pGL4.23 [*luc2*/minP] (Promega, Madison, WI), which contains a gene unspecific minimal promoter sequence (TATA-Box, initiator element, RNA polymerase binding site), and the pGL4.10-*LOXL1* reporter vector containing the specific *LOXL1* core promoter sequence (extending from −1438 bp to the ATG start codon), which was cloned as previously described (17), were used. To test for enhancer activity, an intronic region of 200 bp surrounding rs7173049 (with either A/A or G/G genotype at the polymorphic site) was PCR-amplified with specific primers (Supplementary Material, Table S1) using genomic DNA extracted from human blood samples. The amplified products were cloned into pGL4.10-*LOXL1* and pGL4.23 [*luc2*/minP] vectors via Kpn-I/Bgl-II (New England Biolabs, Ipswich, MA) double digestion and confirmed by sequencing.

For dual luciferase reporter assays hTCF and hTMC were transiently transfected by electroporation using the Nucleofector II transfection device (Lonza, Köln, Germany) and the Amaxa Basic Fibroblasts Nucleofector kit (Lonza) as previously described (17). Depending on the experiment, 5.5 μg of pGL4.10 or pGL4.23 reporter constructs were used together with 0.9 μg Renilla luciferase plasmid pGL4.74 (Promega). Data represent at least three independent experiments for each cell type.

Electrophoresis mobility shift assays

EMSAs were performed as described previously (17). 31 bp synthetic oligonucleotides CCCGGTCAGGACCAC**A**GTGACCATGAGG GCG (rs717-A) and CCCGGTCAGGACCAC**G**GTGACCATGAGGGCG (rs717-G) and their complementary sequences were 5′-labeled with biotin. Both probes included SNP rs7173049 in the center of the probe (Supplementary Material, Table S1). EMSA probes were applied as double strands after paired annealing at 95°C for 5 min followed by cooling down to room temperature for several hours. Nuclear extracts from primary hTCF and hTMC were generated by using a nuclear extraction kit (NE-PER Nuclear and Cytoplasmic Extraction reagents, Thermo Scientific, Bonn, Germany). Each 20 μl binding reaction included either poly(dI·dC) (final concentration: 20 ng/μl) or salmon sperm DNA (final concentration: 5 ng/μl) as non-specific competitor DNA. For supershift assays, 2 μg of antibodies against RXRα (RXRα-1: sc-553X, Santa Cruz Biotechnology, Dallas, TX; RXRα-2: 05-1359, EMD Millipore, Billerica, MA; RXRα-3: sc-46659X), RXRβ (sc-742X), RXRγ (sc-365252X), RARα/β/γ (sc-773X) and THRα/THRβ (MA1–215, Thermo Fisher Scientific, Waltham, MA) was added to the reaction mixture and incubated at room temperature for 30 min prior to addition of the biotinylated probe. As positive control, 500 ng of THRβ recombinant protein (Active Motif, 81120) in binding buffer was incubated with oligonucleotide rs717-G for 20 min in the absence

or presence of anti-THRα/β antibody. For competition experiments, a 100-fold molar excess of unlabeled oligonucleotides were included in the pre-incubation mixture. The resulting complexes were resolved on 6% native polyacrylamide gels (17). EMSA was performed using the Lightshift Chemiluminescent EMSA Kit (Thermo Scientific). Gel shifts were quantitatively analyzed with the LAS-3000 (Fujifilm, Düsseldorf, Germany) chemiluminescence detection system and software (Multi Gauge V3.0, Fujifilm). Data represent at least three biological replicates for each cell type.

CRISPR/Cas9 genome editing

Genome editing of HEK293T cells was done with the Alt-R® CRISPR-Cas9 System components (Integrated DNA Technologies, Coralville, IA) according to the manufacturer's instructions. Two pairs of crRNA (crRNA-F1/R1 and crRNA-F2/R2) with little off-target score were designed (https://benchling.com/) to each delete a 200 bp region flanking rs7173049 using a dual cut approach (Supplementary Material, Table **S1**). Both pairs of crRNA were separately transfected into HEK293T using Lipofectamine® RNAiMAX Transfection Reagent (Thermo Scientific). Transfections with Alt-R® CRISPR-Cas9 Negative Control crRNA #1 served as controls. Single cell-derived clones were isolated using the MoFlo XDP cell sorter (Beckman Coulter, Indianapolis, IN). Screening for positive clones with a homozygous deletion of the target genomic region was performed by using specific primers binding outside the target site (Supplementary Material, Table **S1**) and confirmed by Sanger sequencing.

Real-time PCR

For quantitative real-time PCR ocular tissues and cultured cells were extracted using the Precellys 24 homogenizer and lysing kit (Bertin, Montigny-le-Bretonneux, France) together with the AllPrep DNA/RNA kit (Qiagen, Hilden, Germany) according to the manufacturer's instructions including an on-column DNaseI digestion step using the RNase-free DNase Set (Qiagen). First-strand cDNA synthesis and PCR reaction were performed as previously described (27). Exon-spanning primers (Eurofins Genomics, Ebersberg, Germany), designed with Primer 3 software (http://bioinfo.ut.ee/primer3/), are summarized in Supplementary Material, Table **S1**. Quantitative real-time PCR was performed using the CFX Connect thermal cycler and software (Bio-Rad Laboratories, München, Germany). Probes were run in parallel and analyzed with the ΔΔCt method. Averaged data represents at least three biological replicates. Unique binding was determined with UCSC BLAST search (https://genome.ucsc.edu/), and amplification specificity was checked using melt curve, agarose gel and sequence analyses with the Prism 3100 DNA-sequencer (Applied Biosystems, Foster City, CA). For normalization of gene expression levels, mRNA ratios relative to the house-keeping gene *GAPDH* were calculated.

Immunohistochemistry and immunocytochemistry

Ocular tissue samples were embedded in optimal cutting temperature compound and snap frozen in isopentane-cooled liquid nitrogen. Cryosections of 4 µM thickness were fixed in cold acetone for 10 min, washed in phosphate balanced saline (PBS) and permeabilized using 0.1% Triton X-100 in PBS for 10 min. After blocking with 10% normal goat serum, sections were incubated over night at 4°C in primary antibodies against STRA6 (ab169600, Abcam, Cambridge, UK), ISLR2 (ab81254, Abcam) and LOXL1 (kindly provided by Takako Sasaki, Department of Biochemistry II, Oita University, Japan) diluted in PBS. Antibody binding was detected by Alexa Fluor® 488- or 555-conjugated secondary antibodies (Life Technologies, Carlsbad, CA). Nuclear counterstaining was achieved using 4′,6-diamino-2-phenylindole (DAPI; Sigma-Aldrich, St Louis, MO). Immunolabeled slides and cell cultures were washed and coverslipped with Vectashield mounting medium (Vector Laboratories, Burlingame, CA) prior to evaluation on a fluorescence microscope (BX51, Olympus, Hamburg, Germany). In negative control experiments, the primary antibodies were replaced by equimolar concentrations of isotype-specific mouse and rabbit immunoglobulins or irrelevant isotypic primary antibodies.

Western blot analysis

Total protein was extracted from iris and ciliary body tissues using the Precellys 24 homogenizer and lysing kit (Bertin) with radioimmunoprecipitation assay (RIPA) buffer (50 mM Tris–HCl; pH 8.0; 150 mM NaCl; 1% NP-40, 0.5% sodium deoxycholate (DOC); 0.1% sodium dodecyl sulfate (SDS)). Protein concentrations of ocular tissue preparations, serum and aqueous humor were determined with the Micro-BCA protein assay kit (Thermo Scientific). Proteins were separated by 4–15% SDS-polyacrylamide gel electrophoresis under reducing conditions (6% Dithiothreitol (DTT)) and transferred onto nitrocellulose membranes with the Trans-Blot Turbo transfer system (Bio-Rad Laboratories). Membranes were blocked with SuperBlock T20 (Thermo Scientific) for 30 min and incubated for 1 h at room temperature with polyclonal rabbit antibodies against CRBP1 (ab154881; Abcam) and RBP4 (ab133559; Abcam) diluted 1:2500 and 1:5000, respectively in PBST (0.1% Tween 20 in PBS)/10% SuperBlock T20. Equal loading was verified with mouse anti-human ß-actin antibody (clone AC-15, Sigma-Aldrich) in PBST/10% SuperBlock T20. In negative control experiments, the primary antibody was replaced by PBST. Immunodetection was performed with a horseradish peroxidase-conjugated secondary antibody diluted 1:10000 in PBST/10% SuperBlock T20 and the Super Signal West Femto ECL kit (Thermo Scientific). Band intensity was analyzed with the LAS-3000 (Fujifilm) chemiluminescence detection system and software (Multi Gauge V3.0; Fujifilm).

siRNA silencing

hTCF and hTMC were transiently transfected with specific siRNA (ON-TARGETplus SMARTpool; GE Healthcare Dharmacon, Freiburg, Germany) for *RXRA* (150 pmol; target sequences: GCGC CAUCGUCCUCUUUAA, GCAAGGACCGGAACGAGAA, AGAC CUACGUGGAGGCAAA and UCAAAUGCCUGGAACAUCU) or *THRB* (300 pmol; target sequences: UGGAAGUGUUCGAGGAUUA, GAGAAGAAAUGUAAAGGGU, GGACAAGCACCAAUAGUCA and CGAAAUCAGUGCCAGGAAU) by electroporation using the Nucleofector II transfection device (Lonza) and the Amaxa Basic Fibroblasts Nucleofector Kit (Lonza) with the nucleofector program U-023. Transfections with scrambled siRNA (ON-TARGETplus Non-targeting pool; GE Healthcare Dharmacon) were served as controls. Transfected cells were seeded into 6-well plates in duplicate and harvested at 48 h post-transfection for real-time PCR analysis.

In silico analysis

The PROMO bioinformatics program (http://alggen.lsi.upc.es/cgi-bin/promo_v3/pro-mo/promoinit.cgi?dirDB=TF_8.3) was used to predict transcription factor binding sites affected by SNP rs7173049. The sequences of the genomic region flanking the A allele or G allele of the SNP rs7173049 (±15 bp) were provided as input.

Statistical analysis

Group comparisons were performed using an unpaired two-tailed *t*-test or a Mann–Whitney *U* test using SPSS v.20 software (IBM, Ehningen, Germany). $P < 0.05$ was considered statistically significant.

Supplementary Material

Supplementary Material is available at *HMG* online.

Acknowledgements

The authors thank all patients and healthy subjects for participating in the study. The authors would also like to thank Myriam Eitl, Ekaterina Gedova, Olga Zwenger, Elke Meyer, Angelika Mößner and Petra Koch for excellent technical assistance; Takako Sasaki (Department of Biochemistry II, Oita University, Japan) for the supply of LOXL1 antibody; and the Core Unit Cell Sorting and Immunomonitoring, Erlangen, for cell sorting experiments.

Conflict of Interest statement. The authors declare no competing interests.

Funding

Interdisciplinary Center for Clinical Research at the University Hospital of the University of Erlangen-Nürnberg (Project E23; to A.R. and U.S.S.).

References

1. Konstas, A.G.P. and Ringvold, A. (2018) Epidemiology of exfoliation syndrome. *J. Glaucoma*, **27**, S4–S11.
2. Ritch, R. and Schlötzer-Schrehardt, U. (2001) Exfoliation syndrome. *Surv. Ophthalmol.*, **45**, 265–315.
3. Schlötzer-Schrehardt, U. and Naumann, G.O. (2006) Ocular and systemic pseudoexfoliation syndrome. *Am. J. Ophthalmol.*, **141**, 921–937.
4. Ozaki, M. (2018) Mechanisms of glaucoma in exfoliation syndrome. *J. Glaucoma*, **27**, S83–S86.
5. Ritch, R. (1994) Exfoliation syndrome—the most common identifiable cause of open-angle glaucoma. *J. Glaucoma*, **3**, 176–177.
6. Wirostko, B.M., Curtin, K., Ritch, R., Thomas, S., Allen-Brady, K., Smith, K.R., Hageman, G.S. and Allingham, R.R. (2016) Risk for exfoliation syndrome in women with pelvic organ prolapse : a Utah project on exfoliation syndrome (UPEXS) study. *JAMA Ophthalmol.*, **134**, 1255–1262.
7. Ritch, R. (2016) Systemic associations of exfoliation syndrome. *Asia Pac. J. Ophthalmol. (Phila)*, **5**, 45–50.
8. French, D.D., Margo, C.E. and Harman, L.E. (2012) Ocular pseudoexfoliation and cardiovascular disease: a national cross-section comparison study. *N. Am. J. Med. Sci.*, **4**, 468–473.
9. Besch, B.M., Curtin, K., Ritch, R., Allingham, R. and Wirostko, B.M. (2018) Association of exfoliation syndrome with risk of indirect inguinal hernia: the Utah project on exfoliation syndrome. *JAMA Ophthalmol.*, **136**, 1368–1374.
10. Aung, T., Chan, A.S. and Khor, C.-C. (2018) Genetics of exfoliation syndrome. *J. Glaucoma*, **27**, S12–S14.
11. Dewundara, S. and Pasquale, L.R. (2015) Exfoliation syndrome: a disease with an environmental component. *Curr. Opin. Ophthalmol.*, **26**, 78–81.
12. Thorleifsson, G., Magnusson, K.P., Sulem, P., Walters, G.B., Gudbjartsson, D.F., Stefansson, H., Jonsson, T., Jonasdottir, A., Jonasdottir, A., Stefansdottir, G. *et al.* (2007) Common sequence variants in the LOXL1 gene confer susceptibility to exfoliation glaucoma. *Science*, **317**, 1397–1400.
13. Founti, P., Haidich, A.B., Chatzikyriakidou, A., Salonikiou, A., Anastasopoulos, E., Pappas, T., Lambropoulos, A., Viswanathan, A.C. and Topouzis, F. (2015) Ethnicity-based differences in the association of LOXL1 polymorphisms with pseudoexfoliation/pseudoexfoliative glaucoma: a meta-analysis. *Ann. Hum. Genet.*, **79**, 431–450.
14. Wang, L., Yu, Y., Fu, S., Zhao, W. and Liu, P. (2016) LOXL1 gene polymorphism with exfoliation syndrome/exfoliation glaucoma: a meta-analysis. *J. Glaucoma*, **25**, 62–94.
15. Fan, B.J., Pasquale, L.R., Rhee, D., Li, T., Haines, J.L. and Wiggs, J.L. (2011) LOXL1 promoter haplotypes are associated with exfoliation syndrome in a U.S. Caucasian population. *Invest. Ophthalmol. Vis. Sci.*, **52**, 2372–2378.
16. Hauser, M.A., Aboobakar, I.F., Liu, Y., Miura, S., Whigham, B.T., Challa, P., Wheeler, J., Williams, A., Santiago-Turla, C., Qin, X. *et al.* (2015) Genetic variants and cellular stressors associated with exfoliation syndrome modulate promoter activity of a lncRNA within the LOXL1 locus. *Hum. Mol. Genet.*, **24**, 6552–6563.
17. Pasutto, F., Zenkel, M., Hoja, U., Berner, D., Uebe, S., Ferrazzi, F., Schödel, J., Liravi, P., Ozaki, M., Paoli, D. *et al.* (2017) Pseudoexfoliation syndrome-associated genetic variants affect transcription factor binding and alternative splicing of LOXL1. *Nat. Commun.*, **8**, 15466.
18. Aung, T., Ozaki, M., Lee, M.C., Schlötzer-Schrehardt, U., Thorleifsson, G., Mizoguchi, T., Igo, R.P. Jr., Haripriya, A., Williams, S.E., Astakhov, Y.S. *et al.* (2017) Genetic association study of exfoliation syndrome identifies a protective rare variant at LOXL1 and five new susceptibility loci. *Nat. Genet.*, **49**, 993.
19. Schlötzer-Schrehardt, U. (2009) Molecular pathology of pseudoexfoliation syndrome/glaucoma—new insights from LOXL1 gene associations. *Exp. Eye Res.*, **88**, 776–785.
20. Schlötzer-Schrehardt, U. (2018) Molecular biology of exfoliation syndrome. *J. Glaucoma*, **27**, S32–S37.
21. Mäki, J.M. (2009) Lysyl oxidases in mammalian development and certain pathological conditions. *Histol. Histopathol.*, **24**, 651–660.
22. Schlötzer-Schrehardt, U., Hammer, C.M., Krysta, A.W., Hofmann-Rummelt, C., Pasutto, F., Sasaki, T., Kruse, F.E. and Zenkel, M. (2012) LOXL1 deficiency in the lamina cribrosa as candidate susceptibility factor for a pseudoexfoliation-specific risk of glaucoma. *Ophthalmology*, **119**, 1832–1843.
23. Debret, R., Cenizo, V., Aimond, G., Andre, V., Devillers, M., Rouvet, I., Megarbane, A., Damour, O. and Sommer, P. (2010) Epigenetic silencing of lysyl oxidase-like-1 through DNA hypermethylation in an autosomal recessive cutis laxa case. *J. Invest. Dermatol.*, **130**, 2594–2601.
24. Kleinjan, D.A. and van Heyningen, V. (2005) Long-range control of gene expression: emerging mechanisms and disruption in disease. *Am. J. Hum. Genet.*, **76**, 8–32.

25. Nagasawa, A., Kudoh, J., Noda, S., Mashima, Y., Wright, A., Oguchi, Y. and Shimizu, N. (1999) Human and mouse ISLR (immunoglobulin superfamily containing leucine-rich repeat) genes: genomic structure and tissue expression. *Genomics*, **61**, 37–43.
26. Bouillet, P., Sapin, V., Chazaud, C., Messaddeq, N., Decimo, D., Dolle, P. and Chambon, P. (1997) Developmental expression pattern of Stra6, a retinoic acid-responsive gene encoding a new type of membrane protein. *Mech. Dev.*, **63**, 173–186.
27. Berner, D., Zenkel, M., Pasutto, F., Hoja, U., Liravi, P., Gusek-Schneider, G.C., Kruse, F.E., Schödel, J., Reis, A. and Schlötzer-Schrehardt, U. (2017) Posttranscriptional regulation of LOXL1 expression via alternative splicing and nonsense-mediated mRNA decay as an adaptive stress response. *Invest. Ophthalmol. Vis. Sci.*, **58**, 5930–5940.
28. Kawaguchi, R., Yu, J., Honda, J., Hu, J., Whitelegge, J., Ping, P., Wiita, P., Bok, D. and Sun, H. (2007) A membrane receptor for retinol binding protein mediates cellular uptake of vitamin A. *Science*, **315**, 820–825.
29. Napoli, J.L. (2016) Functions of intracellular retinoid binding-proteins. *Subcell. Biochem.*, **81**, 21–76.
30. Lee, S. and Privalsky, M.L. (2005) Heterodimers of retinoic acid receptors and thyroid hormone receptors display unique combinatorial regulatory properties. *Mol. Endocrinol.*, **19**, 863–878.
31. Ward, L.D. and Kellis, M. (2012) Interpreting non-coding variation in complex disease genetics. *Nat. Biotechnol.*, **30**, 1095–1106.
32. Zhang, F. and Lupski, J.R. (2015) Non-coding genetic variants in human disease. *Hum. Mol. Genet.*, **24**, R102–R110.
33. Maston, G.A., Evans, S.K. and Green, M.R. (2006) Transcriptional regulatory elements in the human genome. *Annu. Rev. Genomics Hum. Genet.*, **7**, 29–59.
34. Smith-Mungo, L.I. and Kagan, H.M. (1998) Lysyl oxidase: properties, regulation and multiple functions in biology. *Matrix Biol.*, **16**, 387–398.
35. Kelly, M. and von Lintig, J. (2015) STRA6: role in cellular retinol uptake and efflux. *Hepatobiliary Surg. Nutr.*, **4**, 229–242.
36. Amengual, J., Zhang, N., Kemerer, M., Maeda, T., Palczewski, K. and Von Lintig, J. (2014) STRA6 is critical for cellular vitamin A uptake and homeostasis. *Hum. Mol. Genet.*, **23**, 5402–5417.
37. Das, B.C., Thapa, P., Karki, R., Das, S., Mahapatra, S., Liu, T.C., Torregroza, I., Wallace, D.P., Kambhampati, S., Van Veldhuizen, P. *et al.* (2014) Retinoic acid signaling pathways in development and diseases. *Bioorg. Med. Chem.*, **22**, 673–683.
38. Gliniak, C.M., Brown, J.M. and Noy, N. (2017) The retinol-binding protein receptor STRA6 regulates diurnal insulin responses. *J. Biol. Chem.*, **292**, 15080–15093.
39. Kelly, M., Widjaja-Adhi, M.A., Palczewski, G. and von Lintig, J. (2016) Transport of vitamin A across blood–tissue barriers is facilitated by STRA6. *FASEB J.*, **30**, 2985–2995.
40. Isken, A., Golczak, M., Oberhauser, V., Hunzelmann, S., Driever, W., Imanishi, Y., Palczewski, K. and von Lintig, J. (2008) RBP4 disrupts vitamin A uptake homeostasis in a STRA6-deficient animal model for Matthew–Wood syndrome. *Cell Metab.*, **7**, 258–268.
41. Pasutto, F., Sticht, H., Hammersen, G., Gillessen-Kaesbach, G., Fitzpatrick, D.R., Nurnberg, G., Brasch, F., Schirmer-Zimmermann, H., Tolmie, J.L., Chitayat, D. *et al.* (2007) Mutations in STRA6 cause a broad spectrum of malformations including anophthalmia, congenital heart defects, diaphragmatic hernia, alveolar capillary dysplasia, lung hypoplasia, and mental retardation. *Am. J. Hum. Genet.*, **80**, 550–560.
42. Chassaing, N., Ragge, N., Kariminejad, A., Buffet, A., Ghaderi-Sohi, S., Martinovic, J. and Calvas, P. (2013) Mutation analysis of the STRA6 gene in isolated and non-isolated anophthalmia/microphthalmia. *Clin. Genet.*, **83**, 244–250.
43. Auffarth, G.U., Blum, M., Faller, U., Tetz, M.R. and Volcker, H.E. (2000) Relative anterior microphthalmos: morphometric analysis and its implications for cataract surgery. *Ophthalmology*, **107**, 1555–1560.
44. Wirostko, B., Allingham, R., Wong, J. and Curtin, K. (2018) Utah project on exfoliation syndrome (UPEXS): insight into systemic diseases associated with exfoliation syndrome. *J. Glaucoma*, **27**, S75–S77.
45. Chen, C.H., Ke, L.Y., Chan, H.C., Lee, A.S., Lin, K.D., Chu, C.S., Lee, M.Y., Hsiao, P.J., Hsu, C., Chen, C.H. and Shin, S.J. (2016) Electronegative low density lipoprotein induces renal apoptosis and fibrosis: STRA6 signaling involved. *J. Lipid Res.*, **57**, 1435–1446.
46. Cvekl, A. and Wang, W.L. (2009) Retinoic acid signaling in mammalian eye development. *Exp. Eye Res.*, **89**, 280–291.
47. Niederreither, K. and Dolle, P. (2008) Retinoic acid in development: towards an integrated view. *Nat. Rev. Genet.*, **9**, 541–553.
48. Bouhenni, R.A., Al Shahwan, S., Morales, J., Wakim, B.T., Chomyk, A.M., Alkuraya, F.S. and Edward, D.P. (2011) Identification of differentially expressed proteins in the aqueous humor of primary congenital glaucoma. *Exp. Eye Res.*, **92**, 67–75.
49. Goodman, A.B. (2006) Retinoid receptors, transporters, and metabolizers as therapeutic targets in late onset Alzheimer disease. *J. Cell Physiol.*, **209**, 598–603.
50. Ramdas, W.D., Wolfs, R.C., Kiefte-de Jong, J.C., Hofman, A., de Jong, P.T., Vingerling, J.R. and Jansonius, N.M. (2012) Nutrient intake and risk of open-angle glaucoma: the Rotterdam study. *Eur. J. Epidemiol.*, **27**, 385–393.
51. Gollapalli, D.R. and Rando, R.R. (2004) The specific binding of retinoic acid to RPE65 and approaches to the treatment of macular degeneration. *Proc. Natl. Acad. Sci. USA*, **101**, 10030–10035.
52. Goodman, A.B. and Pardee, A.B. (2003) Evidence for defective retinoid transport and function in late onset Alzheimer's disease. *Proc. Natl. Acad. Sci. U. S. A.*, **100**, 2901–2905.
53. Ono, K., Yoshiike, Y., Takashima, A., Hasegawa, K., Naiki, H. and Yamada, M. (2004) Vitamin A exhibits potent antiamyloidogenic and fibril-destabilizing effects *in vitro*. *Exp. Neurol.*, **189**, 380–392.
54. Ding, Y., Qiao, A., Wang, Z., Goodwin, J.S., Lee, E.S., Block, M.L., Allsbrook, M., McDonald, M.P. and Fan, G.H. (2008) Retinoic acid attenuates beta-amyloid deposition and rescues memory deficits in an Alzheimer's disease transgenic mouse model. *J. Neurosci.*, **28**, 11622–11634.
55. Kapoor, A., Wang, B.J., Hsu, W.M., Chang, M.Y., Liang, S.M. and Liao, Y.F. (2013) Retinoic acid-elicited RARα/RXRα signaling attenuates Aβ production by directly inhibiting γ-secretase-mediated cleavage of amyloid precursor protein. *ACS Chem. Neurosci.*, **4**, 1093–1100.
56. Jarvis, C.I., Goncalves, M.B., Clarke, E., Dogruel, M., Kalindjian, S.B., Thomas, S.A., Maden, M. and Corcoran, J.P. (2010) Retinoic acid receptor-α signalling antagonizes both intracellular and extracellular amyloid-beta production and prevents neuronal cell death caused by amyloid-β. *Eur. J. Neurosci.*, **32**, 1246–1255.
57. Wang, R., Chen, S., Liu, Y., Diao, S., Xue, Y., You, X., Park, E.A. and Liao, F.F. (2015) All-trans-retinoic acid reduces BACE1

expression under inflammatory conditions via modulation of nuclear factor κB (NFκB) signaling. *J. Biol. Chem.*, **290**, 22532–22542.
58. Rankin, A.C., Hendry, B.M., Corcoran, J.P. and Xu, Q. (2013) An *in vitro* model for the pro-fibrotic effects of retinoids: mechanisms of action. *Br. J. Pharmacol.*, **170**, 1177–1189.
59. Okuno, M., Kojima, S., Akita, K., Matsushima-Nishiwaki, R., Adachi, S., Sano, T., Takano, Y., Takai, K., Obora, A., Yasuda, I. *et al.* (2002) Retinoids in liver fibrosis and cancer. *Front. Biosci.*, **7**, d204–d218.
60. Zhou, T.-B., Drummen, G.P.C. and Qin, Y.-H. (2012) The controversial role of retinoic acid in fibrotic diseases: analysis of involved signaling pathways. *Int. J. Mol. Sci.*, **14**, 226–243.
61. Xiao, W., Jiang, W., Shen, J., Yin, G., Fan, Y., Wu, D., Qiu, L., Yu, G., Xing, M., Hu, G. *et al.* (2015) Retinoic acid ameliorates pancreatic fibrosis and inhibits the activation of pancreatic stellate cells in mice with experimental chronic pancreatitis via suppressing the Wnt/β-catenin signaling pathway. *PLoS One*, **10**, e0141462–e0141462.
62. Dong, Z., Tai, W., Yang, Y., Zhang, T., Li, Y., Chai, Y., Zhong, H., Zou, H. and Wang, D. (2012) The role of all-trans retinoic acid in bleomycin-induced pulmonary fibrosis in mice. *Exp. Lung Res.*, **38**, 82–89.
63. Leem, A.Y., Shin, M.H., Douglas, I.S., Song, J.H., Chung, K.S., Kim, E.Y., Jung, J.Y., Kang, Y.A., Chang, J., Kim, Y.S. *et al.* (2017) All-trans retinoic acid attenuates bleomycin-induced pulmonary fibrosis via downregulating EphA2–EphrinA1 signaling. *Biochem. Biophys. Res. Commun.*, **491**, 721–726.
64. Zhang, C., Kong, X., Ning, G., Liang, Z., Qu, T., Chen, F., Cao, D., Wang, T., Sharma, H.S. and Feng, S. (2014) All-trans retinoic acid prevents epidural fibrosis through NF-κB signaling pathway in post-laminectomy rats. *Neuropharmacology*, **79**, 275–281.
65. Subramanian, U. and Nagarajan, D. (2017) All-trans retinoic acid supplementation prevents cardiac fibrosis and cytokines induced by methylglyoxal. *Glycoconj. J.*, **34**, 255–265.
66. Ohata, M., Lin, M., Satre, M. and Tsukamoto, H. (1997) Diminished retinoic acid signaling in hepatic stellate cells in cholestatic liver fibrosis. *Am. J. Physiol.*, **272**, G589–G596.
67. Aguilar, R.P., Genta, S., Oliveros, L., Anzulovich, A., Gimenez, M.S. and Sanchez, S.S. (2009) Vitamin A deficiency injures liver parenchyma and alters the expression of hepatic extracellular matrix. *J. Appl. Toxicol.*, **29**, 214–222.
68. Barber, T., Esteban-Pretel, G., Marín, M.P. and Timoneda, J. (2014) Vitamin A deficiency and alterations in the extracellular matrix. *Nutrients*, **6**, 4984–5017.
69. Steuer, H., Jaworski, A., Elger, B., Kaussmann, M., Keldenich, J., Schneider, H., Stoll, D. and Schlosshauer, B. (2005) Functional characterization and comparison of the outer blood–retina barrier and the blood–brain barrier. *Invest. Ophthalmol. Vis. Sci.*, **46**, 1047–1053.
70. Coca-Prados, M. (2014) The blood–aqueous barrier in health and disease. *J. Glaucoma*, **23**, S36–S38.
71. Lazar, M.A. (1993) Thyroid hormone receptors: multiple forms, multiple possibilities. *Endocr. Rev.*, **14**, 184–193.
72. Wu, Y., Xu, B. and Koenig, R.J. (2001) Thyroid hormone response element sequence and the recruitment of retinoid X receptors for thyroid hormone responsiveness. *J. Biol. Chem.*, **276**, 3929–3936.
73. Dong, H., Yauk, C.L., Rowan-Carroll, A., You, S.H., Zoeller, R.T., Lambert, I. and Wade, M.G. (2009) Identification of thyroid hormone receptor binding sites and target genes using ChIP-on-chip in developing mouse cerebellum. *PLoS One*, **4**, e4610.
74. Gil-Ibáñez, P., Bernal, J. and Morte, B. (2014) Thyroid hormone regulation of gene expression in primary cerebrocortical cells: role of thyroid hormone receptor subtypes and interactions with retinoic acid and glucocorticoids. *PLoS One*, **9**, e91692.
75. Stoney, P.N., Helfer, G., Rodrigues, D., Morgan, P.J. and McCaffery, P. (2016) Thyroid hormone activation of retinoic acid synthesis in hypothalamic tanycytes. *Glia*, **64**, 425–439.
76. Panza, P., Sitko, A.A., Maischein, H.M., Koch, I., Flotenmeyer, M., Wright, G.J., Mandai, K., Mason, C.A. and Sollner, C. (2015) The LRR receptor Islr2 is required for retinal axon routing at the vertebrate optic chiasm. *Neural Dev.*, **10**, 23.
77. Sauna, Z.E. and Kimchi-Sarfaty, C. (2011) Understanding the contribution of synonymous mutations to human disease. *Nat. Rev. Genet.*, **12**, 683–691.
78. Wang, Z., Boudjelal, M., Kang, S., Voorhees, J.J. and Fisher, G.J. (1999) Ultraviolet irradiation of human skin causes functional vitamin A deficiency, preventable by all-trans retinoic acid pre-treatment. *Nat. Med.*, **5**, 418–422.
79. Challa, P. and Johnson, W.M. (2018) Composition of exfoliation material. *J. Glaucoma*, **27**, S29–S31.
80. Kawaguchi, R., Zhong, M., Kassai, M., Ter-Stepanian, M. and Sun, H. (2015) Vitamin A transport mechanism of the multitransmembrane cell-surface receptor STRA6. *Membranes (Basel)*, **5**, 425–453.
81. Li, H. and Durbin, R. (2009) Fast and accurate short read alignment with Burrows–Wheeler transform. *Bioinformatics*, **25**, 1754–1760.
82. Cirulli, E.T., Lasseigne, B.N., Petrovski, S., Sapp, P.C., Dion, P.A., Leblond, C.S., Couthouis, J., Lu, Y.-F., Wang, Q., Krueger, B.J. *et al.* (2015) Exome sequencing in amyotrophic lateral sclerosis identifies risk genes and pathways. *Science*, **347**, 1436–1441.
83. Do, R., Stitziel, N.O., Won, H.H., Jorgensen, A.B., Duga, S., Angelica Merlini, P., Kiezun, A., Farrall, M., Goel, A., Zuk, O. *et al.* (2015) Exome sequencing identifies rare LDLR and APOA5 alleles conferring risk for myocardial infarction. *Nature*, **518**, 102–106.
84. Auton, A., Brooks, L.D., Durbin, R.M., Garrison, E.P., Kang, H.M., Korbel, J.O., Marchini, J.L., McCarthy, S., McVean, G.A. and Abecasis, G.R. (2015) A global reference for human genetic variation. *Nature*, **526**, 68–74.
85. Howie, B., Fuchsberger, C., Stephens, M., Marchini, J. and Abecasis, G.R. (2012) Fast and accurate genotype imputation in genome-wide association studies through pre-phasing. *Nat. Genet.*, **44**, 955–959.
86. Zenkel, M., Krysta, A., Pasutto, F., Juenemann, A., Kruse, F.E. and Schlötzer-Schrehardt, U. (2011) Regulation of lysyl oxidase-like 1 (LOXL1) and elastin-related genes by pathogenic factors associated with pseudoexfoliation syndrome. *Invest. Ophthalmol. Vis. Sci.*, **52**, 8488–8495.